

Figure 1. A typical cross-section of the GRS RW having a FHR facing for Yamanote Line over Chuo Line in Tokyo, constructed during 1995–2000.

railways and also for roads and other facilities. Any problematic case, including poor performance during severe rains and earthquakes, has not been reported. This type of GRS RW has totally replaced conventional RW types (i.e., gravity type and cantilever RC RWs) and steel strip-reinforced soil RWs with discrete panel facing for new construction of RWs for railways.

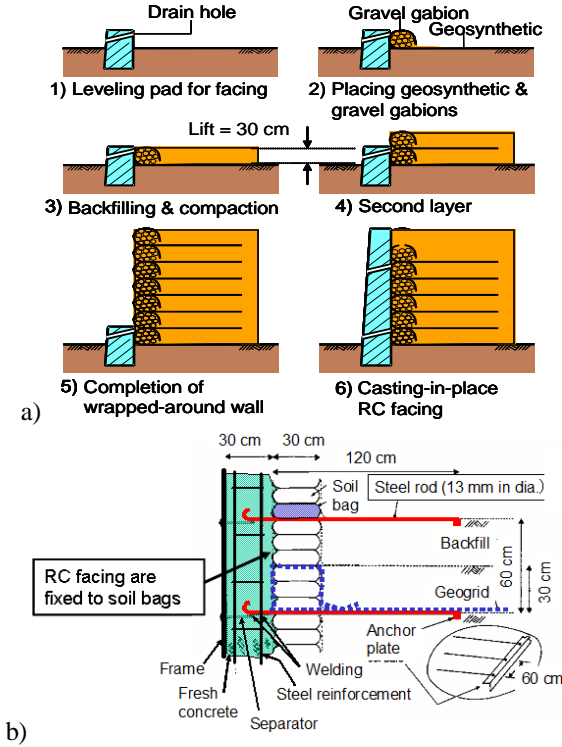


Figure 2. Staged construction of GRS RW: a) construction steps; and b) details of connection between the facing and the reinforced backfill (Tatsuoka et al., 1997, 2007).

The full acceptance of this GRS RW technology by railway engineers is due to a very high cost-effectiveness with a high-seismic stability as validated by high performance during the 1995 Kobe Earthquake (Tatsuoka et al., 1998). This feature was re-confirmed by high performance of a number of GRS RWs of this type that had been constructed for railway including a high-speed train line (Tohoku Shinkan-sen) during the 2011 Great East Japan Earthquake Disaster. On the other hand, a great number of conventional type RWs and embankments on level ground and slopes and in water-collecting places were fully collapsed during these and other earthquakes and heavy rains. Many of them were re-constructed to GRS RWs of this type. The first coastal GRS RW, which is about 10 m high facing Pacific Ocean, was constructed for a length of about 1.0 km in 2010, replacing a gravity type RW that fully collapsed by scouring in the supporting ground during a storm in the summer of 2007 (Tatsuoka & Tateyama, 2012). Based on this technology, coastal dykes and railway and road embankments having

nearly vertical wall faces or sloped slopes consisting of geosynthetic-reinforced backfill with continuous facing connected to the reinforcement layers as tsunami barriers have been proposed.

In this paper, the characteristic features of this GRS RW technology, typical case histories and lessons obtained from their behavior, in particular those during earthquakes and heavy rains, are described.

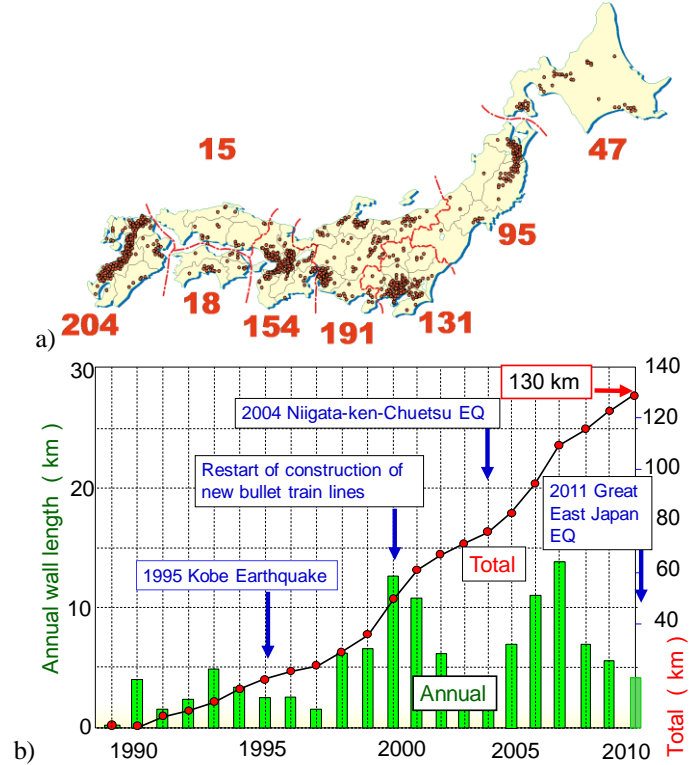


Figure 3. a) Locations; and b) annual and cumulative lengths of GRS RWs with FHR facing (as of March 2011).

1.2 GRS integral and NRS integrated bridges

The second category of innovative GRS structure is a series of new type bridge systems developed based on the technology of GRS-RW with FHR facing, developed to alleviate several serious problems with conventional type bridges (explained later). During the first half of 1990's, a number of GRS bridge abutments were constructed with the girder placed on a pair of sill beams, via a pair of fixed and movable bearings, placed immediately behind the facing on the crest of the reinforced backfill. To alleviate the problems of long-term settlement and unstable behavior during earthquakes of the sill beams, this abutment type was modified by placing the girder on the crest of facings via a pair of bearings (Tatsuoka et al., 2005). Finally, a more innovative bridge system was developed, called the GRS integral bridge, which comprises an integral bridge (with the girder integrated to a pair of RC facings without using bearings) and the backfill reinforced with geosynthetic reinforcement layers connected to the

facings. The GRS integral bridge is much more stable against seismic loads and cyclic lateral displacements at the top of the facing caused by seasonal thermal deformation of the girder. From these features and because of no use of bearings, this bridge is much more cost-effective than the other bridge types described above.

Referring to high cost-effectiveness with high performance of GRS integral bridge, a new method to reinforce existing old conventional type bridges was developed: the backfill is stabilized by large-diameter nails connected to the abutments, then by integrating the girder to the abutments.

2 GRS RETAINING WALLS

2.1 Characteristic features

The three major characteristic features of the GRS RW system (Figs. 1 & 2) are summarised below:

(1) Staged construction procedure (Fig. 2a): The first advantage of the staged construction is that the connection between the reinforcement and the facing is not damaged by differential settlement between the facing and the backfill during wall construction. Then, construction on relatively compressible sub-soil without using heavy piles for the facing and/or using relatively deformable backfill (e.g., on-site soil with a high fines content) becomes possible. Secondly, good compaction immediately at the back of the wall face becomes possible, allowing sufficient outward movements at the wall face mobilizing sufficient tensile forces in the reinforcement during wall construction.

A firm connection between the RC facing and the geosynthetic-reinforced backfill can be ensured as follows (Fig. 2b). Firstly, fresh concrete can easily enter the inside of the gravel-filled soil bags wrapped-around with geogrid reinforcement through the aperture of the geogrid. Secondly, extra water from fresh concrete is absorbed by gravel filling the soil bags, which reduces negative effects of the bleeding phenomenon of concrete. The soil bags function as a temporary but stable facing during construction, resisting against earth pressure generated by compaction works and further backfilling at higher levels. Then, backfill-compaction becomes more effective. The soil bags also function as a drain after construction and as a buffer protecting the connection between the FHR facing and the reinforcement against relative displacement if it takes place after construction. Moreover, to construct a conventional cantilever RC RW, concrete forms on both sides of the facing and its propping are necessary and they become more costly at an increasing rate with an increase in the wall height. With this type of

GRS RW (Fig. 2a), on the other hand, only an external concrete form anchored in the backfill is used without using an external propping is necessary, while not using an internal concrete form (Fig. 2b).

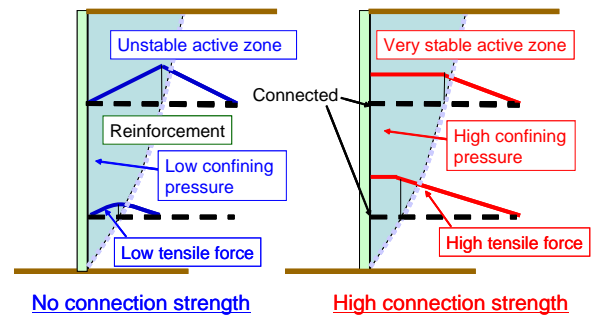


Figure 4. Effects of firm connection between the reinforcement and the facing (Tatsuoka, 1992).

(2) Use of a FHR facing constructed by If the wall face is loosely wrapped-around with geosynthetic reinforcement without using soil bags, or their equivalent, at the shoulder of respective soil layers, or if the reinforcement layers are not connected to a rigid facing, no or only very low tensile forces are activated at the connection between the facing and the reinforcement (Fig. 4a). Then, no or only very small earth pressure is mobilized at the wall face, which results in no significant lateral confining pressure in the active zone. This results in low stiffness and low strength of the active zone, which may lead to intolerably large deformation of the active zone. On the other hand, with this new GRS RW system, the soil bags function as a temporary facing structure and high earth pressure can be activated at the wall face already before placing a FHR facing (Fig. 4b). As the wrapping-around geosynthetic reinforcement at the wall face is buried in the fresh concrete layer (i.e., the facing), eventually the reinforcement layers are firmly connected to the FHR facing. Then, the earth pressure that has been activated on the temporary facing structure comprising soil bags is eventually transferred to the FHR facing. That is, relatively large earth pressure, similar to the active earth pressure that develops in the unreinforced backfill, is activated to the FHR facing, which results in high confining pressure in the active zone, thus high stiffness and strength of the active zone. Then, high performance of the wall can be ensured.

A conventional type RW is a cantilever structure that resists against the active earth pressure from the unreinforced backfill (Fig. 5a). Therefore, large internal moment and shear force is mobilized inside the facing while large overturning moment and lateral thrust force develops at the base of the facing. Thus, a pile foundation is usually used. These disadvantages become more serious at an increasing rate with an increase in the wall height. Relatively large earth pressure, similar to the one activated on the conventional type RW, may be activated on the back

of the FHR facing of the new type GRS RW. Despite the above, as the FHR facing behaves as a continuous beam supported by reinforcement layers at many elevations with a small span, typically 30 cm, small forces are mobilised inside the facing structure (Fig. 5b). Hence, the facing structure becomes much simpler and lighter than conventional cantilever RWs. Besides, the overturning moment and lateral thrust force activated at the facing base becomes small, which makes unnecessary the use of a pile foundation in usual cases. Consequently, the GRS RW having a stage-constructed FHR facing becomes much more cost-effective (i.e., much lower construction cost, much speedy construction using much lighter construction machines) than the conventional type cantilever RC RW.

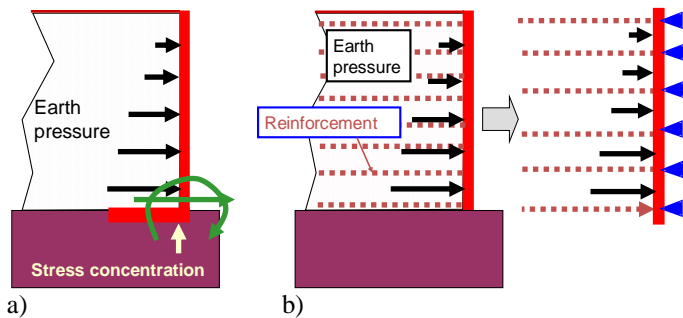


Figure 5. a) conventional type RW; and b) GRS RW with FHR facing (Tatsuoka, 1992, Tatsuoka et al., 1997).

(2) The use of relevant reinforcement type: A polymer geogrid is used for cohesionless soil to ensure good interlocking and a composite of non-woven and woven geotextiles for high-water content cohesive soils to facilitate both drainage and tensile reinforcement. Then, low-quality on-site soil can be used as the backfill if necessary.

(3) The use of relatively short reinforcement: The length of geosynthetic reinforcement necessary for a sufficient stability of GRS RW having staged constructed FHR facing is relatively short when compared to metal strip reinforcement used for walls having discrete panel facing. This is because: 1) the anchorage length of planar geosynthetic reinforcement to resist against the tensile load similar to the tensile rupture strength of reinforcement is much shorter; 2) a FHR facing prevents the occurrence of local failure in the reinforced backfill zone by not allowing the development of failure planes passing through the wall face at an intermediate height; and 3) local failure in the facing, which may take place with discrete panel or block facing and may result in the failure of the whole wall, is difficult to take place with FHR facing. Factors 2) and 3) become more important when concentrated load is applied on the top of, or immediately behind, the facing.



Figure 6. A GRS RW having FHR facing at Tanata, Kobe city; a) immediately after construction; and b) one week after the 1995 Kobe Earthquake (Tatsuoka et al., 1997, 1998).

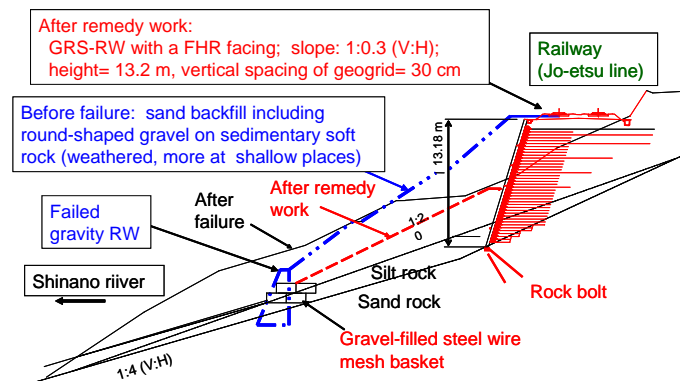


Figure 7. Railway embankment that collapsed during the 2004 Niigata-ken Chuetsu Earthquake and its reconstruction to a GRW RW having FHR facing (Morishima et al., 2005).

2.2 Collapse of RWs and embankments by earthquakes and their reconstruction

Numerous embankments and conventional type RWs collapsed by earthquakes in the past. On the other hand, high performance of a GRS RW having stage-constructed FHR facing during the 1995 Kobe Earthquake (Fig. 6) validated its high-seismic stability. Many gently sloped embankments and conventional type RWs that collapsed by that and subsequent earthquakes were reconstructed to GRS RWs of this type (Tatsuoka et al., 1977, 1998; 2007; Koseki et al., 2006, 2008; Koseki, 2012). Typically, three railway embankments supported by gravity type RWs on slope collapsed during the 2004 Niigata-ken Chuetsu Earthquake and they were reconstructed to GRS RWs of this type (Fig. 7). The adoption of this technology was due to not only much lower construction cost and much higher stability (in

particular for these soil structures on steep slopes) but also much faster construction resulting from a significant reduction of earthwork when compared to the original gently sloped embankment with a gravity type RW.

Based on vast and very serious damage to railway structures during the 1995 Kobe Earthquake, the seismic design codes for railway structures were substantially revised (Tatsuoka et al., 2010a). The revised codes for soil structures have following several new concepts and procedures:

- 1) Introduction of very high design seismic loads (i.e., level 2) and three ranks of required seismic performance.
- 2) Recommendation for the use of geosynthetic-reinforced soil structures.
- 3) Evaluation of seismic performance based on residual displacement.
- 4) Use of peak and residual shear strengths with well compacted backfill, while ignoring apparent cohesion due to suction assuming that it fully disappears during heavy rains.
- 5) Design based on the limit equilibrium stability analysis.
- 6) An emphasis of good backfill compaction and good drainage.
- 7) No creep reduction factor applied to obtain the rupture strength of geosynthetic reinforcement in seismic design.

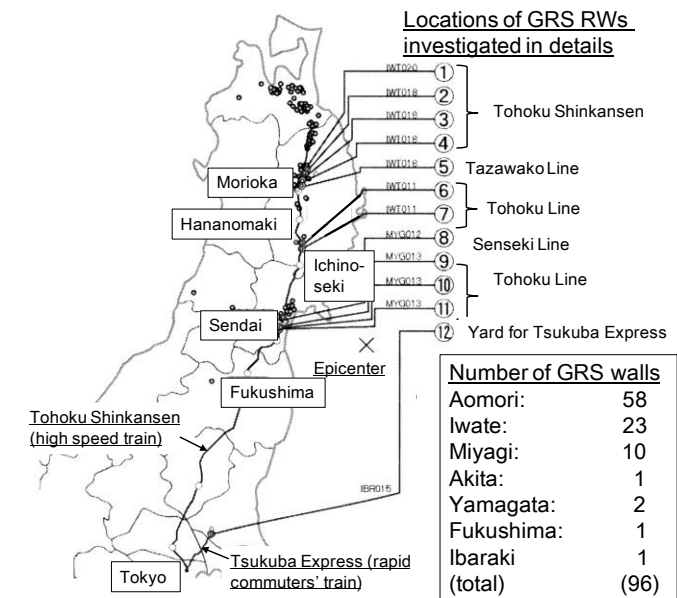


Figure 8. Locations and numbers of GRS RWs having FHR facing for railways constructed before the 2011 Great East Japan Earthquake Disaster (Tateyama, 2012).

The 2011 Great East Japan Earthquake Disaster, which took place 11th March, is the most disastrous earthquake in Japan after the World War II. The damage was a combination of those from earthquake motions and the accompanying great tsunami. A great number of old embankments and RWs that

were not designed and constructed following the current seismic design standard collapsed. In comparison, a number of GRS RWs of this type that had been designed based on the revised seismic design code described above and constructed in the affected areas of this earthquake performed very well (Fig. 8),

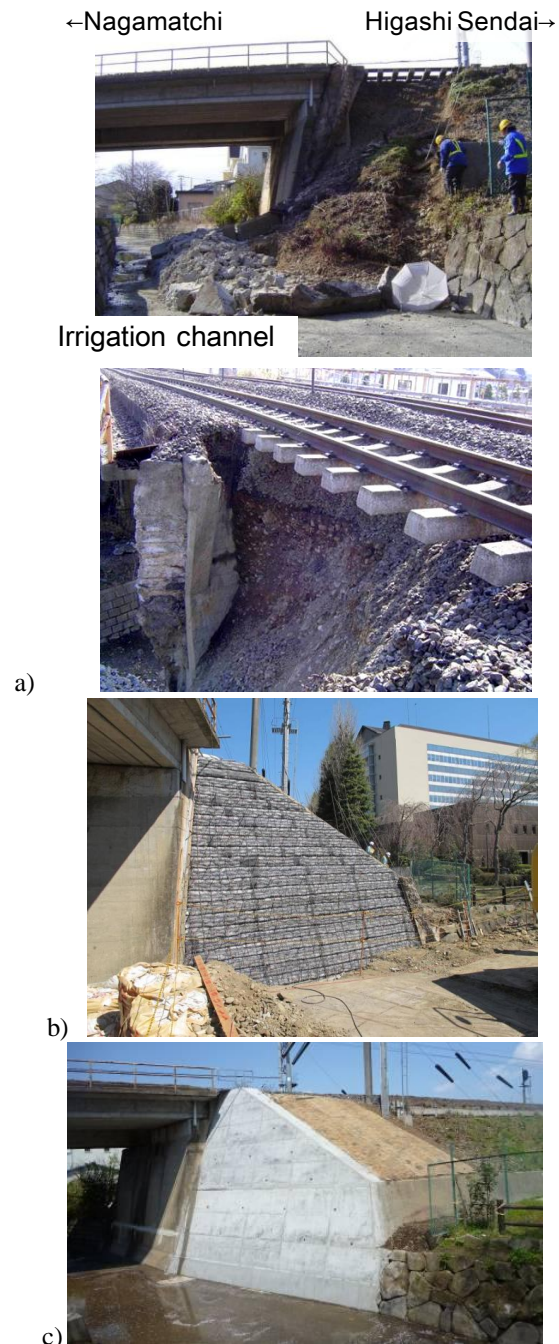


Figure 9. a) Collapse of a wing RW (with a masonry facing of a bridge abutment) at site No. 11 in Fig. 8 (Nagamachi, Sendai for Tohoku Freight line); and b) & c) its reconstruction to a GRS RW (by the courtesy of the East Japan Railway Co.).

Several conventional type RWs and embankments that collapsed were reconstructed to GRS RWs of this type (Fig. 9). A very fast construction was one of the important advantages of this technology also in this case. In particular, the railway was re-opened at a restricted speed before constructing a FHR fac-

ing (Fig. 9b). Fig. 10 shows one of the three embankments that collapsed during an earthquake induced one day after the Great East Japan Earthquake Disaster and reconstructed to GRS RWs of this type.

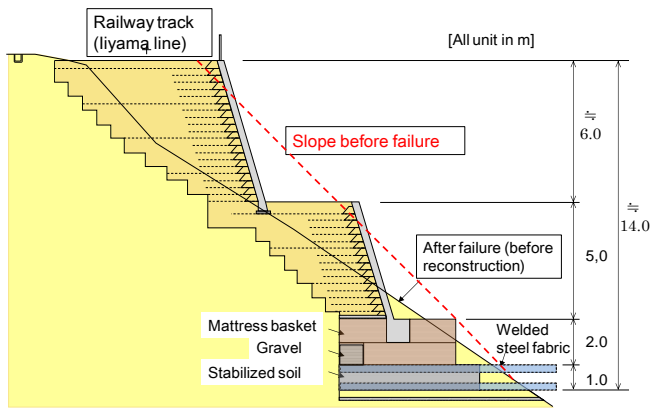


Figure 10. One of the three embankments between Yokokura and Morinomiya stations, Iiyama Line, that collapsed during the Nagano-Niigata Border Earthquake and reconstructed to GRS RWs (by the courtesy of the East Japan Railway Co.)

2.3 Collapse of RWs and embankments by heavy rains, floods and storms and reconstruction

Numerous embankments and conventional type RWs collapsed also by heavy rains, floods and storms in the past. GRS RWs (Fig. 2) were also constructed to replace a number of embankments that were eroded and washed away by over-flowing flood water (Tatsuoka et al., 1997, 2007). Numerous embankments for roads and railways retained by gravity-type RWs along rivers and seashores collapsed by floods and storms, usually triggered by over-turning failure of the RWs caused by scouring in the supporting ground (Fig. 11a). The backfill is largely eroded resulting in the stop of the function of a railway or a road. This type of collapse is easy to take place, because the conventional type RW is a cantilever structure of which the stability is fully controlled by the bearing capacity at the bottom of the RW.

On the other hand, GRS-RWs with a FHR facing is not such a cantilever structure as above, therefore, much more stable against scouring in the supporting ground (Fig. 11b). It is particularly important that the major part of the backfill can survive even if the supporting ground is scoured. A high embankment retained by a masonry gravity-type RW at the lower part on the left bank of Agano river, Niigata Prefecture, for West Ban-Etsu line (a railway of East Japan Railway) was collapsed by a flood 30th July 2011 by the mechanism illustrated in Fig. 11a. It was reconstructed to an about 9.4 m-high and 50 m-long GRS RW with a FHR facing (Fig. 12).

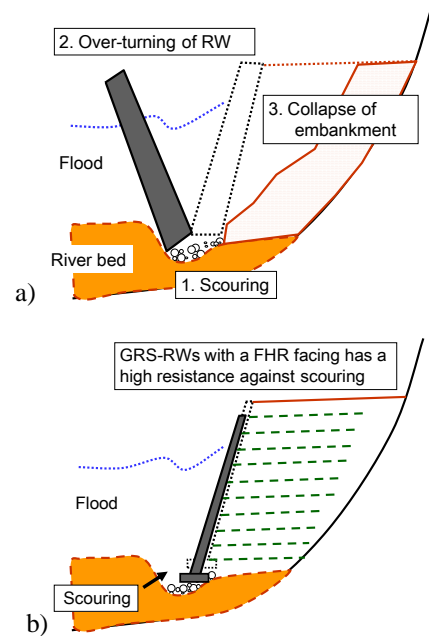


Figure 11. a) Collapse of conventional type RW by scouring in the subsoil (the numbers show the sequence of events); and b) improved performance of GRS-RW with FHR facing.

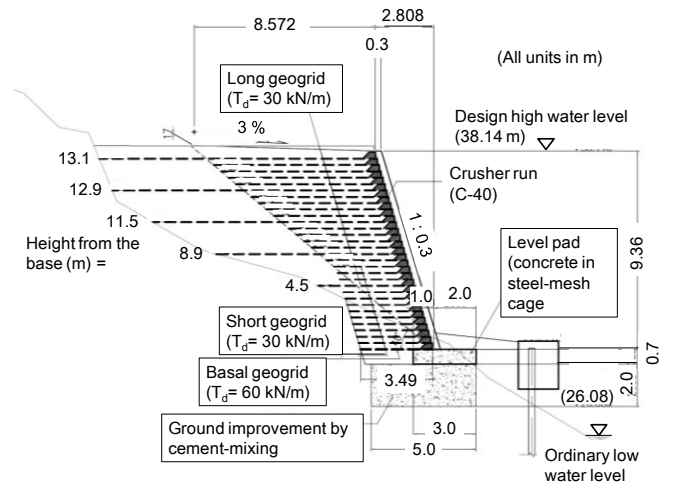
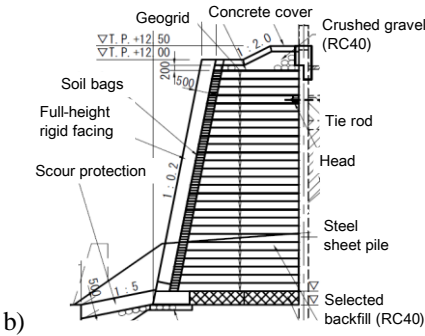


Figure 12. Reconstruction of RW on the left bank of Agano river, Niigata Prefecture, for West Ban-Etsu line to a GRS-RW (by the courtesy of the East Japan Railway Co.).

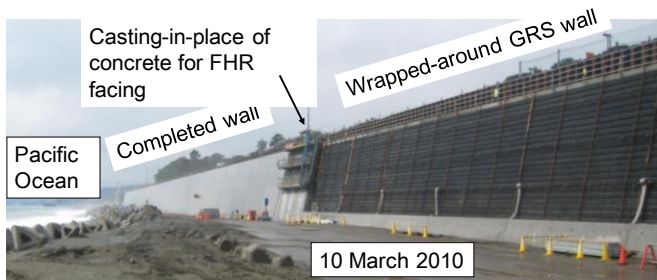
Fig. 13 shows another case of this type of failure of a gravity-type RW for a length of about 1.5 km along seashore facing the Pacific Ocean, triggered by scouring in the supporting ground by strong ocean waves during a typhoon No. 9, 29th Aug. 2007. The wall was reconstructed to a GRS RW with FHR facing (Figs. 13b & c). The FHR facing has a strong resistance against sea wave actions during storms, while the wall could be stable even if the supporting ground is scoured to some extent. On the other hand, discrete panel facing is not relevant in such a case as this, because the loss of the stability of a single or several panel(s) by scouring in the subsoil and/or erosion of the backfill from joints between adjacent panels may easily lead to the failure of the whole wall.



a)



b)



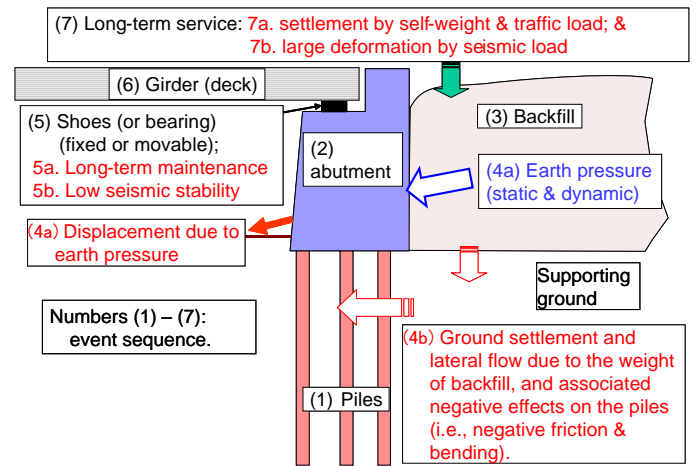
c)

Figure 13. Seawall for Seisho by-pass of National Road No. 1 in Kanagawa Prefecture, southwest of Tokyo: a) collapse for a length of about 1.5 km by Typhoon No. 9, 29th Aug. 2007; b) a typical cross-section of GRS RW; and c) GRS RW under construction (a & b: by the courtesy of the Ministry of Land, Infrastructure, Transport and Tourism).

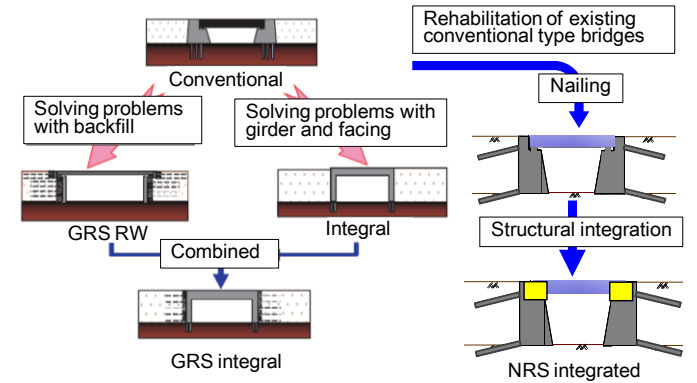
3 NEW BRIDGE TYPES

3.1 Problems with conventional type bridges

A conventional type bridge usually comprises a single simple-supported girder supported by a pair of abutments via fixed (or hinged) and moveable bearings, or multiple simple-supported girders supported by a pair of abutments and a single or multiple pier(s) via multiple sets of bearings. The approach fill is usually unreinforced backfill. The abutment may be a gravity structure (unreinforced concrete or masonry) or a RC structure. The conventional type bridge has a number of drawbacks as described below (Fig. 14a).



a)



b)

Figure 14. a) Several major problems with conventional type bridges; and b) development of new bridge types for new construction and reinforcement (Tatsuoka et al., 2008a, b; 2009).

Firstly, as the abutment is a cantilever structure retaining unreinforced backfill, the earth pressure induces large internal forces as well as large thrust forces and overturning moment at its bottom. This problem becomes more serious when designed against severe earthquake loads. Therefore, usually the abutment becomes massive and a pile foundation becomes necessary more at an increasing rate with an increase in the abutment height. Secondly, although only very small movement is allowed with the abutments, the backfill are constructed after the abutments have been completed. Hence, when constructed on thick soft ground, many long piles may become necessary to prevent any small movement of the abutments caused by the earth pressure as well as settlement and lateral flow in the subsoil. Large negative friction may develop along the piles. Thirdly, the construction and long-term maintenance of the bearings and the connections between simple-supported girders are generally costly. Fourthly, the bearings and the backfill are the weakest elements against seismic loads. The girder may dislodge at a moveable bearing by severe seismic loads. A significant bump may be formed behind the abutment by long-term settle-

ment of the backfill due to its self weight, traffic loads and seismic loads.

3.2 Integral bridge and GRS RW bridge

To alleviate the problems with the conventional type bridge (Fig. 14a), several new bridge types have been proposed (Fig. 14b), which are either for new construction or for reinforcement of existing old bridges. For new construction, the integral bridge comprises the girder structurally integrated to the facings without using bearings. This bridge type was developed to alleviate problems with the structural part (i.e., the girder and facings) of the conventional type bridge. This bridge type is now widely used for roads in the UK, the USA and Canada due mainly to a lower cost for construction and maintenance resulting from no use of bearings and the use of a continuous girder.

However, as the backfill is not reinforced, thus not integrated to the abutments (or facings), the backfill and the structural part do not help each other. Hence, this bridge type cannot alleviate some old problems with unreinforced backfill (described above). Moreover, as the girder is integrated to the abutments, seasonal thermal expansion and contraction of the girder results in cyclic lateral displacements at the top of the abutments, which may result in: i) development of high passive earth pressure on the back of the facing; and ii) large settlements due to active failure in the backfill (England et al., 2000). The test results showing the above are presented later.

A number of bridges comprising a pair of GRS RWs with FHR facing that supports a simple-supported girder via bearings placed on sill beams on the crest of the backfill immediately behind the facing were constructed (i.e., GRS RW bridges; Tatsuoka et al., 1997, 2005). Although this bridge type is more cost-effective than the conventional type, the length of the girder is restricted due to low stiffness of the backfill supporting the sill beams and a low seismic stability of the sill beams because of their small mass. Then, this type was modified by placing a girder on the top of the FHR facings via bearings (Fig. 13a; Tatsuoka et al., 2005, 2009). The first prototype was completed in 2003 for a new bullet train line in Kyushu (Fig. 15b). The abutment was constructed by the staged construction procedure, following the GRS RW technology (Fig. 2). That is, the geosynthetic-reinforced backfill is first constructed, followed by the construction of the facing by casting-in-place fresh concrete. Then a girder was placed on the top of a thin RC facing via bearings. In this case, a trapezoidal-shaped zone of backfill back of the facing was a well-compacted cement-mixed well-graded gravelly soil to minimize the long-term residual deformation and to ensure a very high seismic stability. The conventional type RC

abutment laterally supports the unreinforced backfill and the backfill activates static and dynamic earth pressures on the abutment. In contrast, with this new type abutment, the reinforced backfill laterally supports a thin RC facing, therefore, the backfill does not activate large earth pressure on the facing. After this project, nearly sixty similar bridge abutments were designed or constructed until today. Despite the above, this type of abutment is not free from several problems due to the use of bearings.

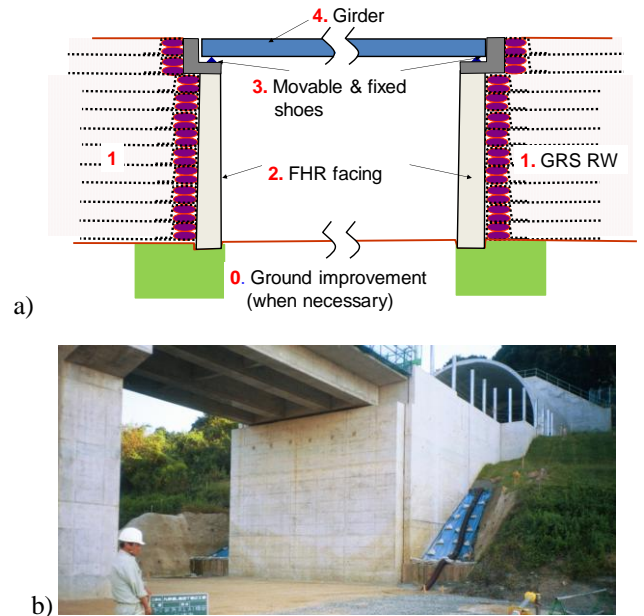


Figure 15. a) GRS RW bridge with the girder placed on the top of the facing via bearings (n.b., the numbers denote the construction sequence); and b) first prototype at Takada, Kyushu, for a new bullet train line (Tatsuoka et al., 2005, 2009).

3.3 GRS integral bridge

To alleviate all these serious drawbacks with conventional type bridge and also those with integral bridges and GRS RW bridges, summarized above, the authors proposed a new bridge type for new construction, called the Geosynthetic-Reinforced Soil (GRS) integral bridge (Fig. 14a; Tatsuoka et al., 2008a, b, 2009, 2012a). This bridge type comprises a girder integrated to a pair of FHR facings (without using bearings) and backfill reinforced with geosynthetic layers connected to the facings. This type of bridge is staged-constructed as follows, referring to Fig. 16a:

- 0) When the supporting ground is soft and weak, the subsoil below the abutments may be improved by, for example, cement-mixing in-place.
- 1) A pair of GRS walls with the wall face wrapped-around with geogrid reinforcement is constructed.
- 2) After major deformation of the supporting ground and backfill has taken place, thin RC abutments (i.e., FHR facings) are constructed by

casting-in-place fresh concrete on the wall face wrapped-around with geogrid reinforcement, in the same way as GRS retaining walls with FHR facing (Fig. 2a: Tatsuoka et al., 1997).

- 3) A continuous girder is constructed structurally integrated to the top of the facings.

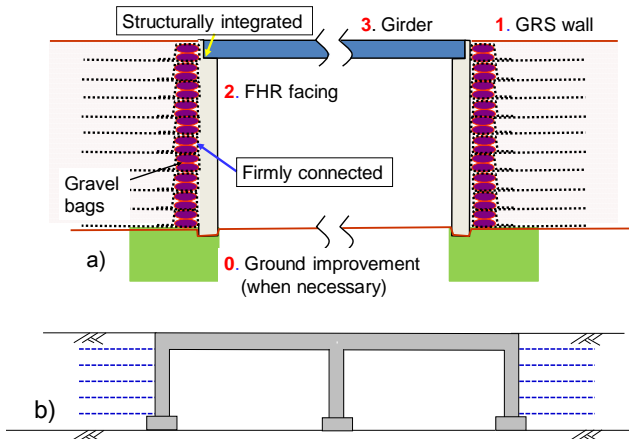


Figure 16 GRS integral bridge: a) construction sequences denoted by the numbers; and b) two-span bridge.

With conventional type bridges and GRS RW bridges, the length of a single girder is restricted to avoid excessive lateral seismic loads to be activated on the abutment on which a fixed bearing supports the girder. With integral bridges, the girder length is restricted additionally to avoid excessive large cyclic lateral displacements at the top of the facings by seasonal thermal deformation of the girder. The girder length of conventional type integral bridge is presently specified to be 50 - 60 m in the USA to restrict the maximum thermal deformation of the girder to about 10 cm. With the GRS integral bridge, such restrictions as above are looser and its girder length limit would be larger than the value for the conventional type integral bridge. Fig. 16b illustrates a GRS integral bridge having two spans.

3.4 NRS integrated bridge

There exist a great number of old conventional type bridges with the girder placed on the abutments via a pair of bearings, that are judged not to satisfy the seismic stability requirement according to the current design standard. Due to deterioration with time, the number of such bridges as above is increasing every year. It is extremely time-consuming and costly to replace such a bridge with a new one without closing a road or a railway, because the following complicated procedure is necessary: 1) a temporary bridge is constructed adjacent to the existing bridge together with constructing a new approach railway or road; 2) the existing bridge is removed; and 3) a new bridge is constructed at the place of the old bridge; and 4) the temporary bridge is removed.

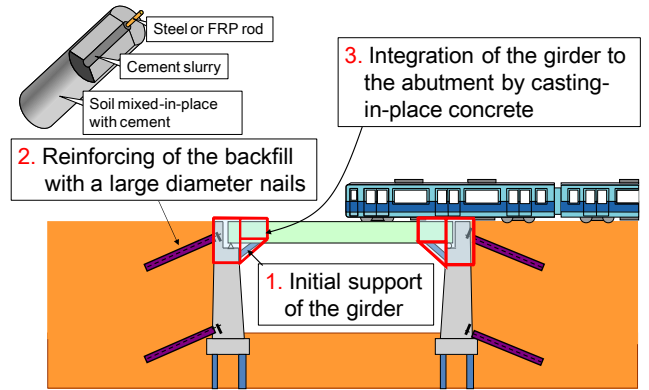


Figure 17. A new method to reinforce old conventional type bridges (n. b., the numbers denote the construction sequence).

The authors proposed to reinforce such existing old conventional type bridges as described above by taking advantage of structural characteristics of GRS integral bridges (Shiranita et al., 2010; Tatsuoka et al., 2012b). This reinforcement method is illustrated in Fig. 17:

1. The girder is initially supported with a steel elbow member.
2. The backfill is reinforced with a large-diameter nail (typically 40 cm in diameter), which comprises a tie rod (steel or FRP) surrounded with the backfill mixed-in-place with cement-slurry provided from a central hollow rod containing the tie rod (Tateyama et al., 1996). The nails are connected to the top and bottom of the abutment.
3. The girder is integrated to the abutments by placing casting-in-place concrete.

The bridge reinforced by this technology is called the nail-reinforced soil (NRS) integrated bridge. This technology has two major advantages. Firstly, the existing bridge is reinforced while in service, thus this method is much faster and much cheaper than the replacement with a new bridge. Secondly, the NRS integrated bridge is much more stable than the conventional type bridge because of no use of bearings and reinforcement of the backfill.

To validate the advantages of GRS integral bridge and NRS integrated bridge, a series of static cyclic loading tests and shaking table tests were performed on small models in 1g, as described below. In 2009, full-scale models of GRS integral bridge and NRS integrated bridge were constructed. A high constructability of these bridge types was confirmed. In the beginning of 2011, full-scale loading tests of these two bridge models were performed.

4. STATIC CYCLIC LOADING TESTS

4.1 GRS integral bridge

Fig. 18 shows the setup of small model tests in the laboratory performed to simulate lateral cyclic dis-

placements at the top of the abutment (or the facing) by seasonal thermal deformation of the girder.

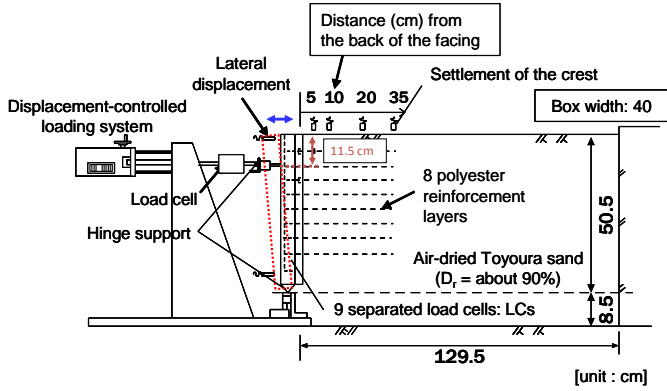


Figure 18. Model tests to evaluate negative effects of lateral cyclic displacements at the top of the abutment (i.e., facing): this figure is when the backfill is reinforced (Tatsuoka et al., 2009).

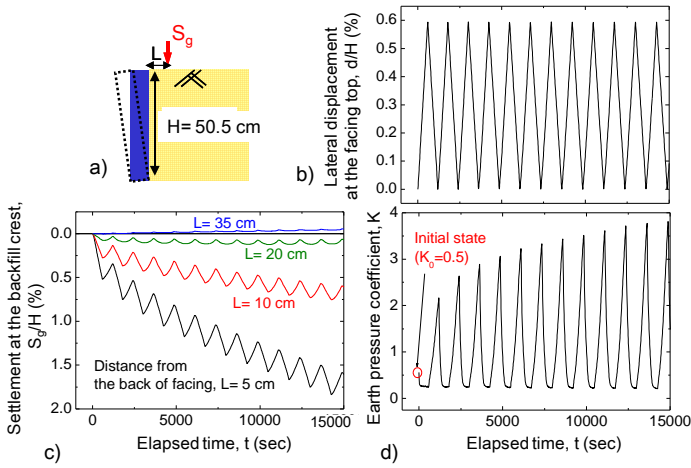


Figure 19. a) Loading method; and measured time histories of b) horizontal displacement at the facing top, c) backfill settlement; and d) total earth pressure, unreinforced dense Toyoura sand ($D_r = 90\%$) (Tatsuoka et al., 2009).

Fig. 19 shows the result of a typical test when the backfill is not reinforced and the facing is hinged at the bottom. The top of the facing is displaced cyclically on the active side. Despite a fixed relatively small amplitude of displacement, with cyclic loading, the earth pressure that increases when the facing is displaced in the passive direction continues increasing and the settlement in the backfill that takes place when the facing is displaced in the active direction continues increasing, both without showing a sign of stopping. Eventually, active failure takes place in the backfill, while the earth pressure becomes close to the large passive pressure.

Tatsuoka et al. (2009, 2010b) showed that these trends of behavior are due to the dual ratchet mechanism in the backfill (Fig. 20a). That is, only the active mode of deformation develops when the facing moves in the active direction and it accumulates with cyclic loading, while only the passive mode of deformation develops when the facing moves in the

passive direction and it accumulates with cyclic loading. Fig. 20b illustrates the stress-strain behavior on the active failure plane and passive failure plane during cyclic displacements of the facing. Due to the dual ratchet mechanism, although the facing displaces with the same amplitude, the shear strain consistently increases on both AFP and PFP, which eventually result into active failure and high passive earth pressure.

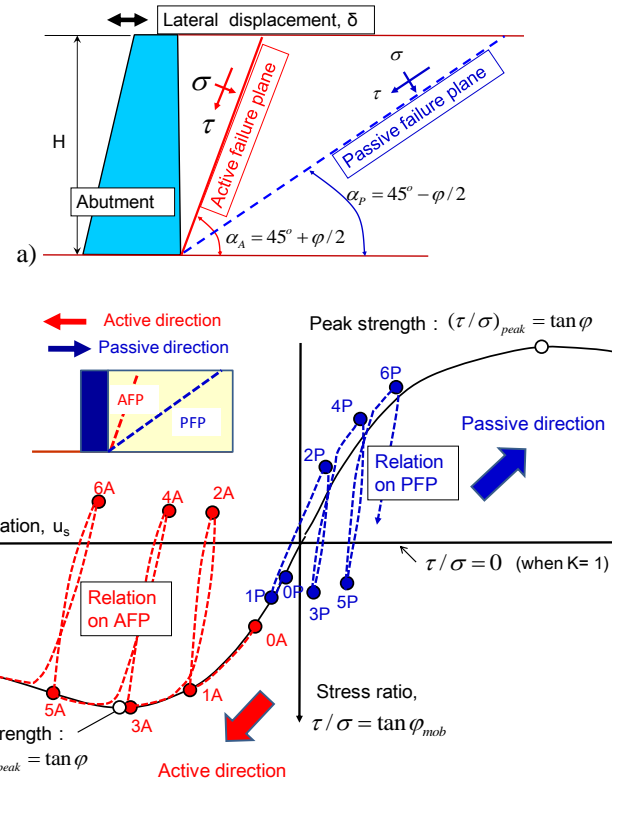


Figure 20. a) Backfill behind an abutment with vertical smooth face and a horizontal backfill crest; and b) stress-strain behaviors on AFP and PFP (Tatsuoka et al., 2010b).

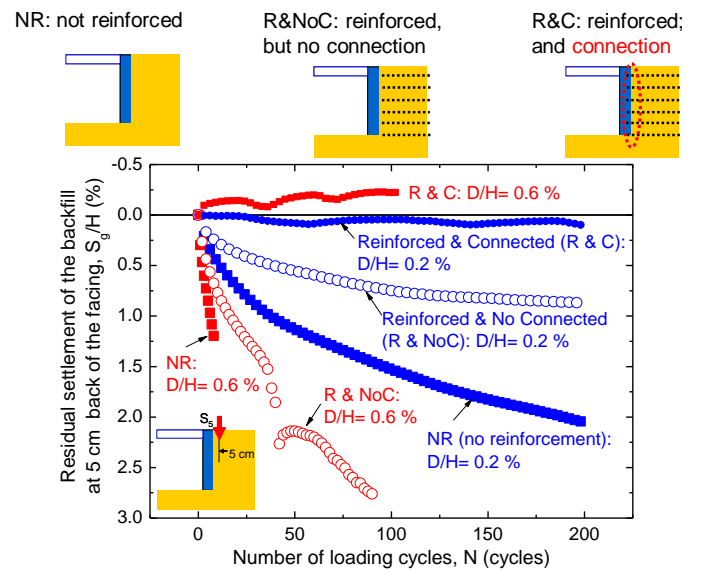


Figure 21. Effects of reinforcing of the backfill with geosynthetic reinforcement connected to the facing on the settlement in the backfill by lateral cyclic loading of the facing (Tatsuoka et al., 2009).

The result when the backfill is unreinforced and the facing displacement D/H is 0.6 % presented in Fig. 21, together with a similar test result when $D/H=0.2\%$, are summarized in Fig. 21. The results when the backfill is reinforced with and without connected to the facing are also presented in Fig. 21. It may be seen that the active failure in the backfill can be effectively prevented by reinforcing the backfill with the geogrid layers connected to the facing. When the geogrid layers are not connected to the facing, the settlement is still very large. The passive earth pressure increases even when the backfill is reinforced with geogrid connected to the facing. Even so, the stability of the facing is kept, as the facing is supported by a number of geogrid layers.

4.2 NRS integrated bridge

A series of similar tests as those presented above for the IGS integral bridge were performed on small models of the abutment of NRS integrated bridge (Fig. 22; Tatsuoka et al., 2012b). To highlight the effects of nailing, the abutment model was embedded only to a depth of 3 m in the supporting ground, simulating prototype abutments not supported with any pile foundation.

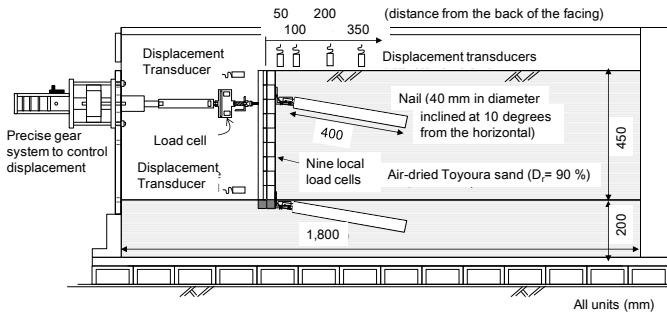


Figure 22. Static lateral cyclic loading tests on an abutment model with nails in the backfill and supporting ground (Tatsuoka et al., 2012b).

Fig. 23a compares the settlement ratio, S/H , at 5 cm from the abutment, where H is the height of the abutment model (48 cm), plotted against the number of loading cycle, N , when the backfill and supporting ground was unreinforced or nailed. Fig. 21b compares the outward lateral displacement ratio at the abutment bottom, d/H . Without nailing, distinct active failure took place in the backfill with very large settlements even when D/H was as small as 0.2 %. Besides, due to the development of large passive earth pressure, the abutment bottom was largely pushed out, which restrained the development of high passive earth pressure. These trends became more significant with an increase in the cyclic lateral displacement at the abutment top, D/H . With nails

connected to the top and bottom of the abutment, the active displacement at the abutment footing became essentially zero and the active failure in the backfill was effectively restrained, then the settlement in the backfill became much smaller. Yet, the settlement is not very small due to separated arrangements of nails in the backfill. Some additional measure is necessary to minimize the backfill settlement. Relatively high passive pressure developed because the dual ratchet mechanism was still somehow active in spite of nailing. However, the abutment supported by the nails was kept stable.

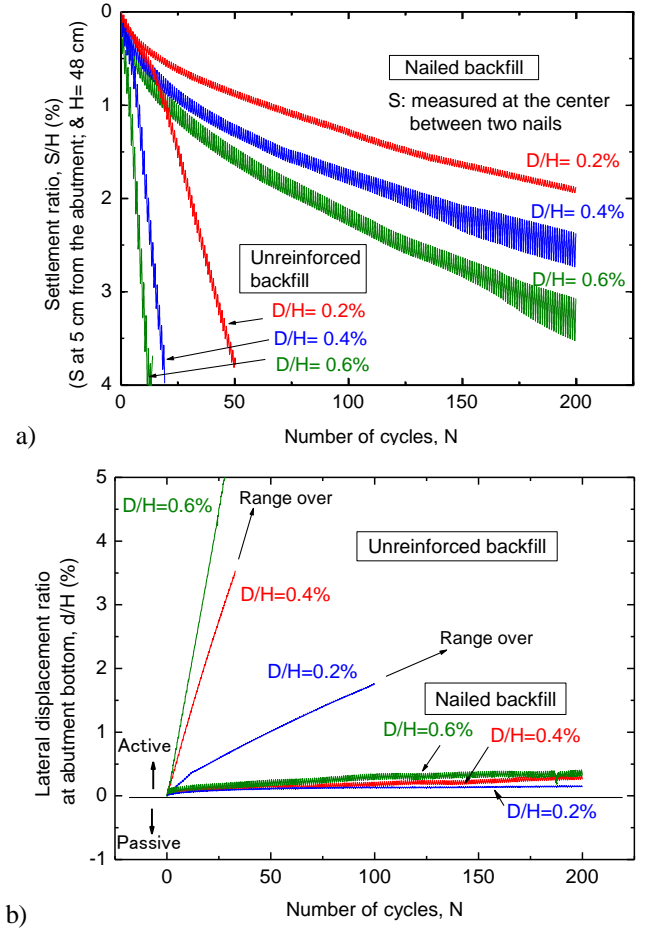


Figure 23. a) Settlement ratio; and b) lateral displacement ratio at the abutment bottom, plotted against the number of cycle in the cases with and without nailing (Tatsuoka et al., 2012b).

In summary, the abutment and backfill of a conventional type bridge become very stable against cyclic lateral displacements caused by seasonal thermal expansion and contraction of the girder by reinforcing the backfill and supporting ground with nails connected to the top and bottom of the abutment. When further the girder is integrated to the abutments, the seismic stability increases substantially, as shown below.

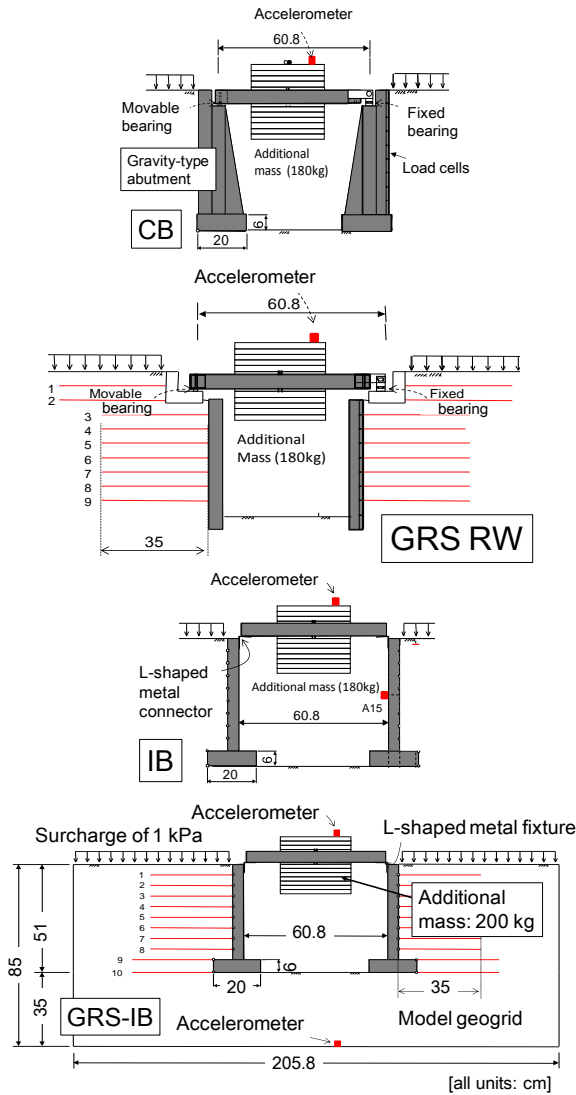


Figure 24. Models for shaking table tests (n. b., the whole model is shown only with GRS-IB) (Muñoz et al., 2012).

5. SHAKING TABLE TESTS

5.1 GRS integral bridge

The following four models were tested (Fig. 22):

CB (conventional type bridge): A pair of gravity type abutments (without a pile foundation) supported the girder via fixed and movable bearings (a hinge and a roller). The backfill was unreinforced air-dried Toyoura sand ($D_r = 90\%$). Due to a space limitation in the sand box, an additional mass was attached to the girder to simulate a 2 m-long girder. The length scale of the model relative to the assumed prototype was 1/10.

GRS-RW (geosynthetic-reinforced soil retaining wall bridge): A pair of sill beams supporting the girder via fixed and movable bearings was placed on the crest of GRS RWs having a FHR facing.

IB (integral bridge): The model was the same as GRS-IB except that the backfill was not reinforced.

GRS-IB (GRS integral bridge): The girder is connected to the facings with a pair of L-shaped metal fixtures (20 cm-long, 5 cm-wide and 3 mm-thick),

which did not exhibit the major resisting moment. The backfill was reinforced with grid reinforcement layers connected to the facing. Two other models with a cement-mixed backfill zone immediately behind the facing (GRS-IB-C and GRS-IB-C-T) were also prepared. The details are reported in Tatsuoka et al. (2009).

In the first series of shaking tests (on these models described in Fig. 24), twenty sinusoidal waves at a frequency f_i of 5 Hz was exerted to the shaking table at each stage increasing the acceleration level incrementally by 100 gals (i.e., cm/sec^2) until the models collapsed. In the second series (on models IB and GRS-IB), input motions at various frequencies were used to examine whether the conclusions from the first series is relevant for a wide range of f_i .

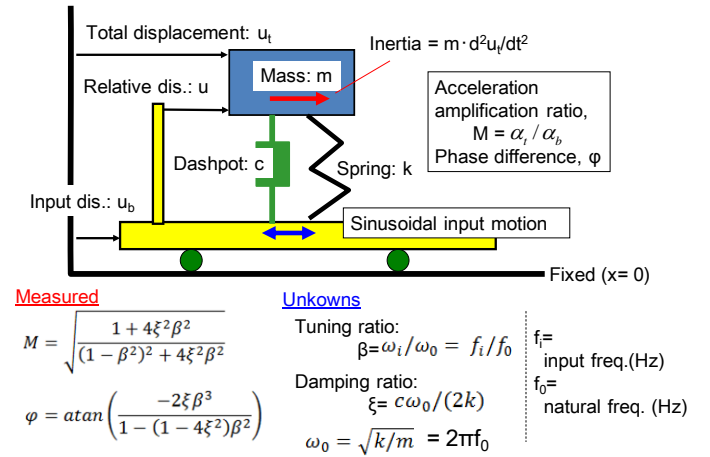


Figure 25. Damped SDOF system.

The observed dynamic behaviours of the bridge models were analyzed by assuming a damped single-degree-of-freedom (SDOF) system (Fig. 25). From the amplification ratio M ($=$ the ratio of the response acceleration at the girder (α_t) to the input acceleration (α_b)) and the phase difference φ between α_t and α_b observed in every cycle, the tuning ratio β ($=$ the ratio of the input frequency (f_i) to the transient natural frequency (f_0)) and the transient damping ratio ξ were back-calculated. With each model, the value of β decreased and the value of ξ increased with an increase in the number of loading cycle N at the same input acceleration (α_b) and with an increase in α_b , as typically seen from Figs. 26 - 28. These trends were different among the different models due to their different nonlinear load-deformation properties (Munoz et al., 2012). In the first series, all the models started failing when the resonant state was reached. Then, the β value increased exceeding the unity and eventually collapse took place.

The test results showed that the response acceleration for a given input motion decreases and the possibility to reach the resonant state decreases: 1) with an decrease in the initial value of β (i.e., with an increase in the initial value of f_0 , representing the initial stiffness of the structure); and 2) with a decrease

in the increasing rate of β (i.e., the decreasing rate of f_0) associated with an increase in N and α_b . Furthermore, 3) for a given input motion, the response acceleration decreases with an increase in the damping ratio. Finally, 4) the maximum response acceleration at which the model starts failing increases with an increase in the structural strength. It is shown below that the GRS integral bridge has advantages in all of these factors, therefore, it exhibits a very high seismic stability.

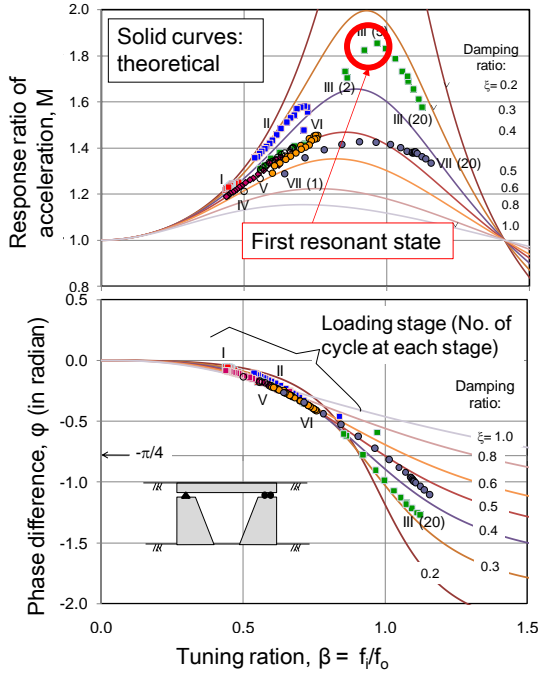


Figure 26. Response of model CB ($f_i = 5$ Hz): I, II denote loading stages; and the numerals in () denote the number of cycle at each stage (Muñoz et al., 2012).

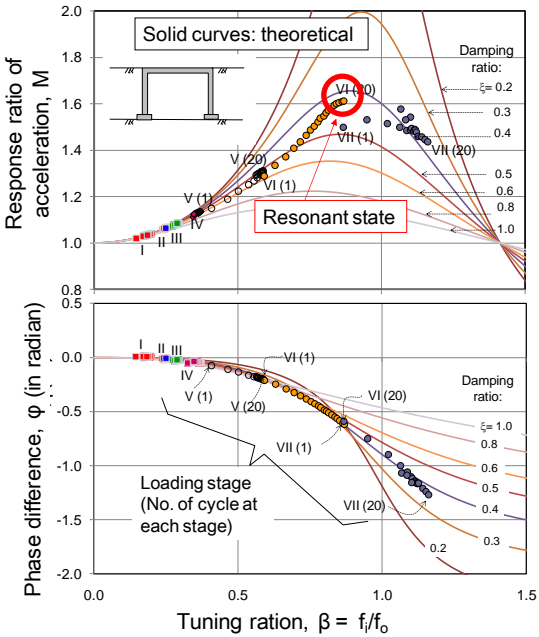


Figure 27. Response of model IB (Muñoz et al., 2012).

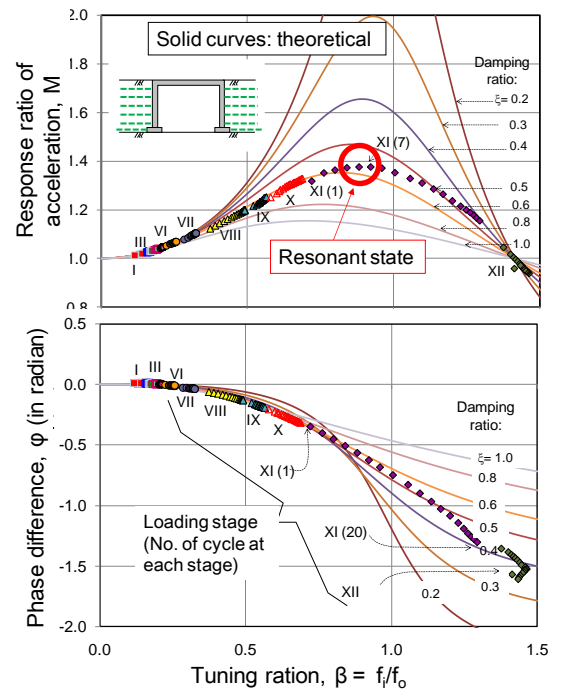


Figure 28. Response of model GRS-IB ($f_i = 5$ Hz) (Muñoz et al., 2012)

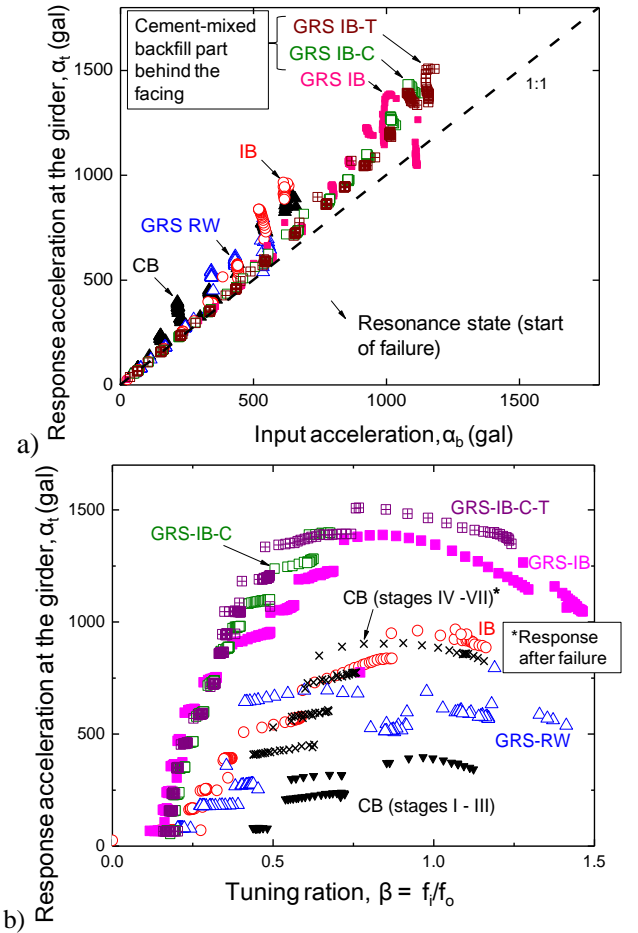


Figure 29. Responses of four bridge models ($f_i = 5$ Hz) (Muñoz et al., 2012)

Fig. 29a shows the relationship between the input and response accelerations, α_t and α_b . With CB, $M = \alpha_t/\alpha_b$ started increasing at the smallest α_b , because of the largest initial value of β and the largest increas-

ing rate of β (i.e., the largest decreasing rate of f_0) with dynamic loading, as seen from Fig. 30. In Figs. 26 - 20, the multiple data points at the same input acceleration α_b with each model denote an increase in β due to a decrease in the f_0 value with an increase in the number of loading cycles (up to 20). An increase in β resulted in an increase in M , therefore an increase in α_t (Fig. 29b). Besides, with CB, the strength, defined as the response acceleration at which failure started, was smallest while the damping ratio at failure was smallest (Fig. 31). Consequently, CB reached the resonant state fastest and the collapse took place at the smallest α_b .

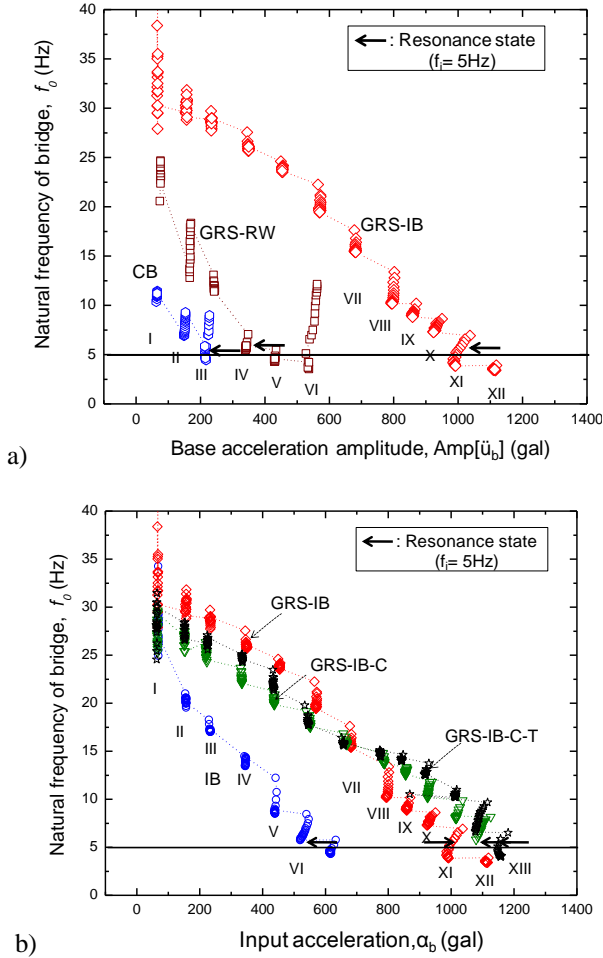


Figure 30. Decrease in f_0 with an increase in the input acceleration of four bridge models ($f_i = 5$ Hz) (Muñoz et al., 2012).

On the other hand, with GRS IB, the initial value of β was smallest (i.e., the initial value of f_0 was largest) and the increasing rate of β (i.e., the decreasing rate of f_0) was smallest (Fig. 30), while the damping ratio at failure was largest and the strength was largest (Fig. 31). Consequently, GRS IB reached the resonant state most slowly and the collapse took place at the largest α_b (Fig. 31). This very high performance of GRS IB is due all to integration of the girder, the facing and the backfill. The performance of models GRS-RW bridge and integral bridge (IB) was intermediate due to their intermedi-

ate levels of structural integration. As seen from Figs. 29 - 31, the dynamic performance of GRS IB was improved slightly by arranging a cement-mixed backfill zone immediately behind the facing.

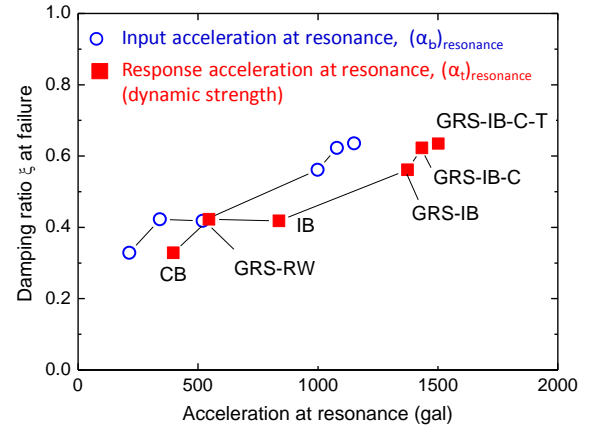


Figure 31. Accelerations and damping ratios at the start of failure (i.e., at resonance) of six bridge models ($f_i = 5$ Hz) (Muñoz et al., 2012).

As seen from Fig. 31, the damping ratio, ξ , at the start of failure increases with an increase in the dynamic strength and the ξ value of model GRS IB is much higher than model CB. This is because, with an increase in the structural integration among the girder, facing and backfill, the material damping at the start of failure of: i) the material damping of the backfill and supporting ground as part of the bridge system; and ii) the dynamic energy of the girder and abutments dissipated via wave propagation toward the outside of the bridge system increase.

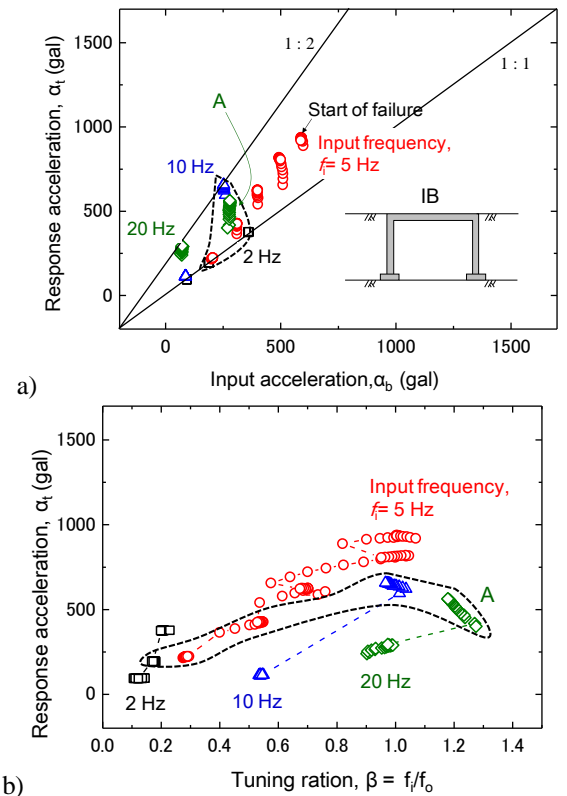


Figure 32. Response of model IB ($f_i = 2 \sim 20$ Hz).

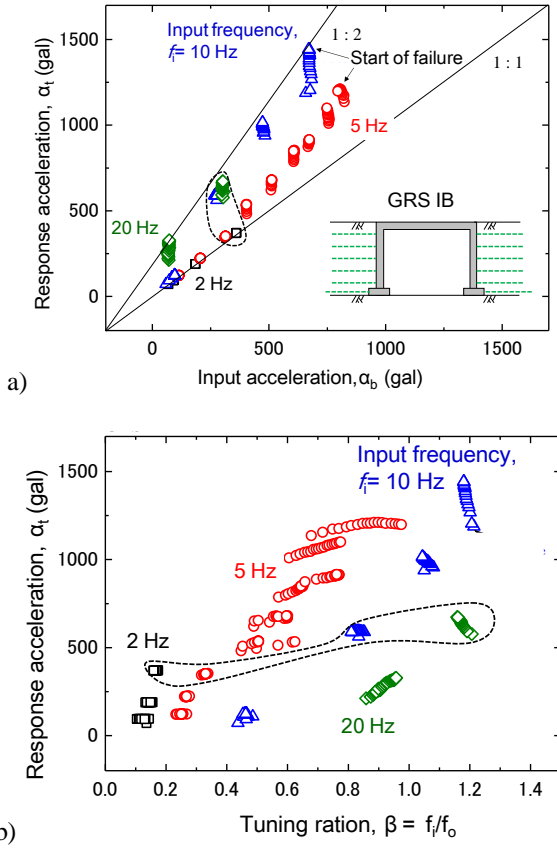


Figure 33. Response of model GRS IB ($f_i = 2 \sim 20$ Hz).

Figs. 32 and 33 show the results from the second series on models IB and GRS IB, in which the input acceleration a_b was increased changing the input frequency f_i at respective stages. In each figure, the data plotted in a broken circle denote the responses at different f_i values for the nearly same a_b . For the same f_0 value, the β value increases with an increase in f_i , which results in an increase in the M value before the resonant state is reached and a decrease in M after the resonant state has been passed (i.e., the case denoted by A in Fig. 32). Therefore, with an increase in f_i , the resonant state is reached at a lower a_b and it becomes more likely to pass the resonant state without collapse taking place. It may also be seen from Figs. 32 and 33 that, not only at $f_i = 5$ Hz but also at other f_i values, the M value increases with an increase in β associated with an increase in the number of loading cycle and a_b ; and GRS IB was much more dynamically stable than IB.

Fig. 34 shows acceleration spectra for a wide range of damping ratio ξ of a typical very severe ground earthquake motion. The aseismic design of RC and steel structures is usually based on a response spectrum for $\xi = 5\%$, which is considered representative of the value at failure of these types of super-structure. On the other hand, the ξ value of model GRS IB reached as high as 60% at the start of failure (Fig. 31). Therefore, the response spectra for ξ up to 70% are also depicted in Fig. 34. The initial value (before the start of seismic loading) of the

natural period T_0 of ordinary prototype bridges, including ordinary GRS integral bridges, is shorter than the predominant period T_p of severe earthquake motions, which is about 0.35 second in the case of Fig. 34: i.e., the initial value of the natural frequency f_0 is higher than the predominant frequency $f_p = 1/T_p$ (= about 3 Hz). The implications of the shaking table test results are discussed below based on Fig. 34 by assuming that similar response spectrum are kept during a given major earthquake motion.

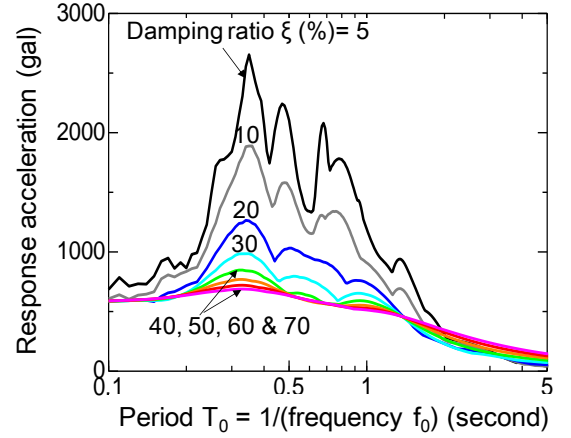


Figure 34. Acceleration response spectra for different damping ratios of NS component of the earthquake motion recorded at JMA Kobe, 1995 Kobe Earthquake (by the courtesy of Dr Izawa, J., RTRI Japan).

With GRS integral bridges, when compared with the other bridge types examined in the present study, the initial value of $\beta = f_p/f_0$ ($\ll 1.0$) is lower, which means a lower initial value of the natural period T_0 ($=1/f_0$) ($\ll T_p$), which results in a lower initial response acceleration. Besides, the increasing rate of β is lower, which means a lower increasing rate of T_0 . Then, the chance to reach the resonant state becomes lower. Furthermore, as the ξ value at failure is very high, even if having reached the resonant state, the response acceleration is kept very low. When $\xi = 60\%$, the M value at resonance is about 1.35 for the stationary sinusoidal input motions (Figs. 26a – 29a). In the case of Fig. 34, the magnification ratio M at resonance for an irregular input motion defined as the ratio of the response acceleration at $T_0 = T_p$ to the value at $T_0 = 0.0$ (at which $M = 1.0$) is also around 1.35. This observation indicates that the design response acceleration at the girder of a GRS integral bridge can be set to be substantially lower than ordinary RC and steel structure (e.g., a bridge girder supported by RC piers). Besides, it is reasonable to set the design maximum response acceleration at the girder of GRS integral bridges to be lower than the other bridge types, despite a much higher strength. Based on the above, a design M value between 1.0 and 1.35 is reasonable for such a GRS integral bridge as the one examined in these shaking table tests. Yet, it is necessary to examine whether and how the damping ratio at the start of failure decreases-

es with an increase in the girder weight under otherwise the same conditions.

5.2 NRS integrated bridge

The following five models (Fig. 35) were prepared by reinforcing the conventional type bridge model (CB) (Fig. 22a):

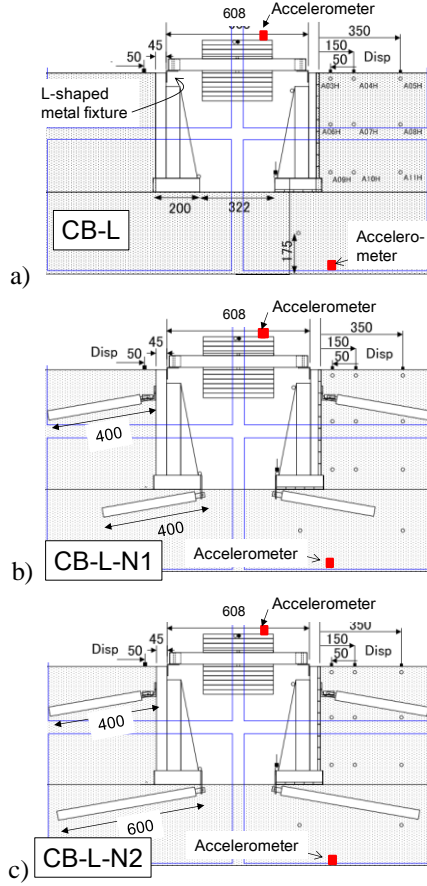


Figure 35. Small models of conventional type bridge reinforced in different ways for shaking table tests, only visible zones through windows (denoted by solid lines) presented (all units are in mm: Tatsuoka et al., 2012b).

CB-L (integrated conventional type bridge): The girder was integrated to a pair of gravity-type abutments of model CB using a pair of L-shaped metal fixtures. The backfill was unreinforced air-dried Toyoura sand ($D_r = 90\%$).

CB-L-N1 (integrated CB with nailing): The backfill and part of supporting ground of model CB-L was reinforced with two layers of 40 cm-long nails on each side. Two nails of each top layer were connected to the top of the abutment and two of each bottom layer to the footing toe of the abutment via pin connectors. The model nails were a hollow circular brass rod with a diameter of 4 cm, modeling a full-scale large-diameter nail with a diameter of 40 cm based on a length scale factor of 10. The surface of the model nail was made rough by gluing Toyoura sand particles.

CB-L-N2: The length of the bottom nails (40 cm) of model CB-L-N1 were made longer to 60 cm to increase the pull-out strength. This model exhibited the highest dynamic stability among those tested in the present study.

Although two other models similar to CB-L-N2 were tested (Tatsuoka et al., 2012b), the results are not presented herein due to page limitations. Two series of tests were performed. In the first series on all the models described above, twenty sinusoidal waves at a frequency f_i of 5 Hz was exerted to the shaking table at each stage increasing the acceleration level incrementally by 100 gals. In the second series on model CB-L-N2, input motions at various frequencies were used. The observed dynamic behaviours of the models were analyzed by the theory of the SDOF system (Fig. 25). A typical analysis is presented in Fig. 36. In this test, the shaking was ceased before reaching the resonant state due to the capacity of the shaking table.

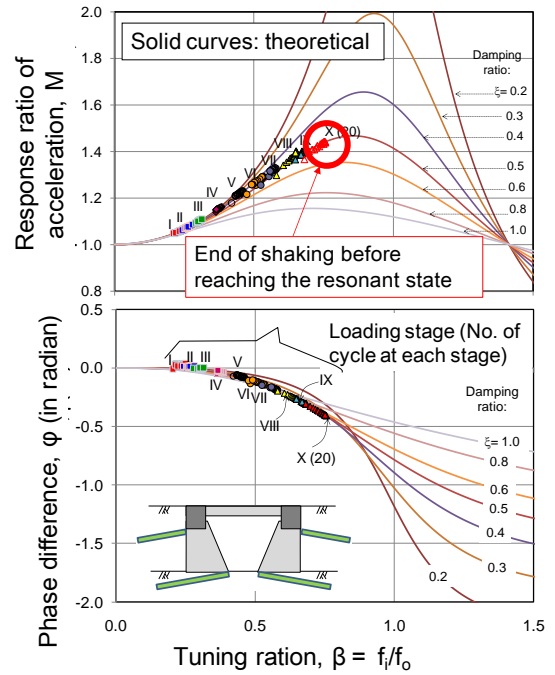


Figure 36. Response of model CB-L-N2 ($f_i = 5$ Hz).

From the results from series 1 (Figs. 36 – 39), it may be seen that, by integrating the girder to the abutments and further by nailing the backfill and part of the subsoil, i) the initial β value decreased (i.e., the initial value of the natural frequency f_0 increased); ii) the increasing rate of β (i.e., the decreasing rate of f_0) decreased; iii) the response acceleration at resonance, at which failure started; increased; and iv) the damping ratio at the start of failure increased, all contributing to a substantial increase in the dynamic stability. It may also be seen that the dynamic stability increased by using longer nails. Tatsuoka et al. (2012b) reported that connecting the bottom nails to the foundation toe of the

abutment (as models CB-L-N1 and N2) is essential to maintain the contact of the bottom of the footing with the subsoil, thereby to maintain a high dynamic stability.

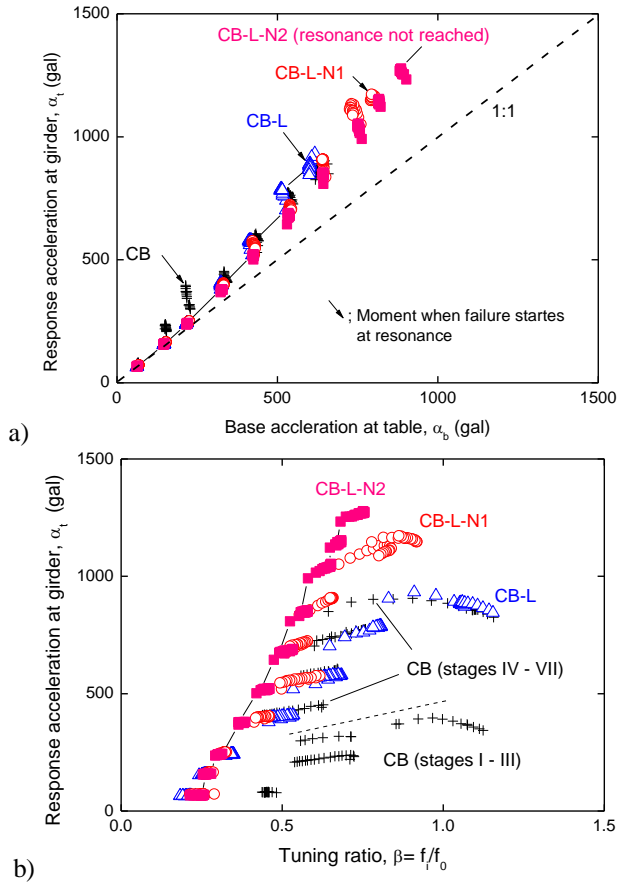


Figure 37. Responses of five bridge models ($f_i = 5$ Hz).

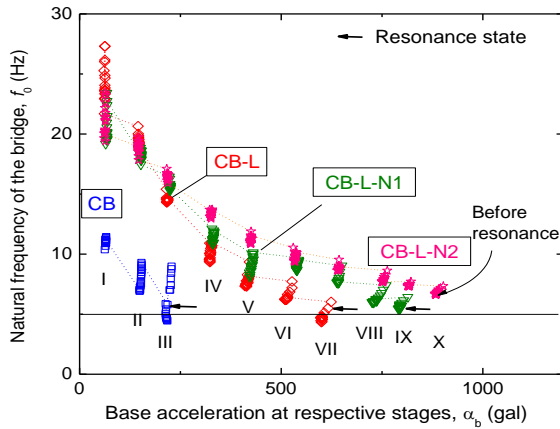


Figure 38. Decrease in the natural frequency with an increase in the input acceleration of four bridge models ($f_i = 5$ Hz).

The behavior of model CB-L-N2 for various input frequencies (series 2) is presented in Fig. 40. It may be seen that the magnification of acceleration changes by changes in the tuning ratio, β , in the course of dynamic loading in the same way as series 1. This means that the conclusions from series 1, described above, are relevant also for a wide range of f_i .

In summary, it can be concluded that the dynamic stability of conventional type bridge can be substantially improved by the reinforcing technology de-

picted in Fig. 17 (i.e., the NRS integrated bridge) to the similar level as GRS integral bridge (Fig. 16).

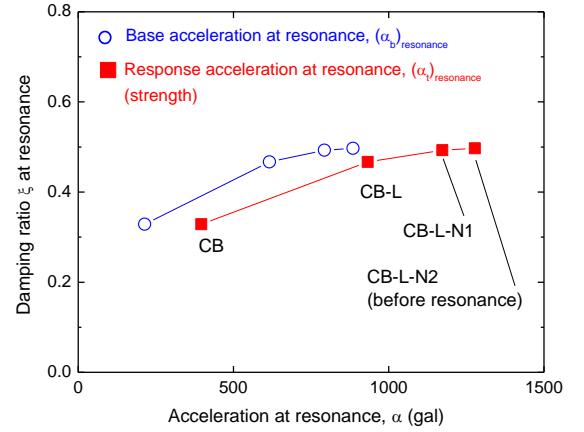


Figure 39. Accelerations and damping ratios at the start of failure (i.e., at resonance) of four bridge models ($f_i = 5$ Hz).

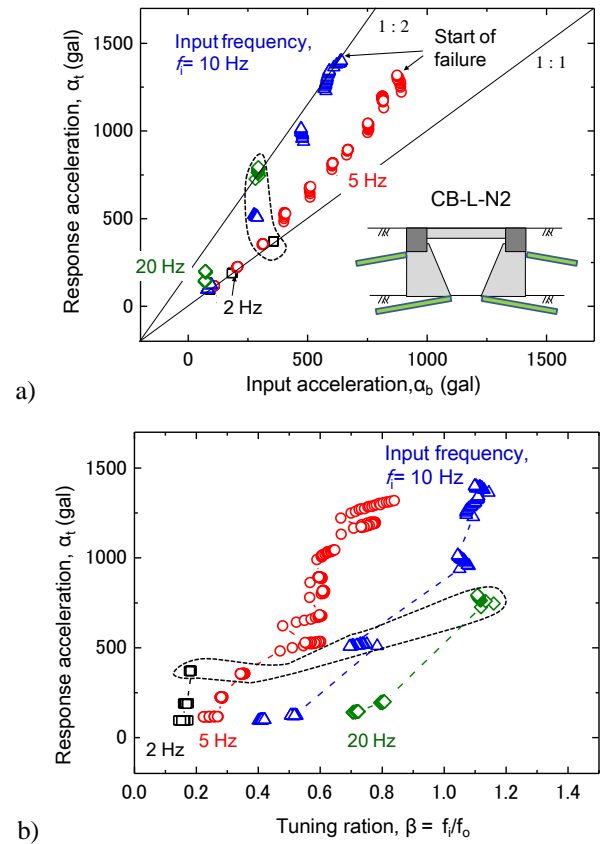


Figure 40. Response of model CB-L-N2 ($f_i = 2 \sim 20$ Hz).

3.3 Dynamically brittle versus ductile behaviour

Tatsuoka et al. (1988) reported the performance of various types of retaining wall (RW) during the 1995 Kobe Earthquake. Based on the above and those from a series of shaking table tests, they concluded that the dynamic behaviour of gravity-type RWs with unreinforced backfill is generally dynamically very brittle in the sense that the failure starts at a relatively low ground acceleration and full collapse may quickly take place subsequently. On the other hand, the dynamic behaviour of GRS RWs with a FHR facing (Fig. 2) is dynamically ductile in the

sense that the failure starts at a relatively high ground acceleration and full collapse may take place only after a relatively large increase in the ground acceleration. Based on the above, they proposed to use a higher design seismic coefficient in the quasi-static limit equilibrium-based stability analysis with gravity type RWs than with GRS RWs under otherwise the same conditions.

However, they did not show the mechanism for brittle and ductile behaviours of RWs. The results from the shaking table tests shown above indicate that:

- 1) the dynamic behaviour of conventional type bridge is indeed dynamically brittle while the one of GRS integral and NRS integrated bridges is ductile; and
- 2) the dynamically brittle or ductile behaviour of soil structures results from: a) a low or high initial value of the natural frequency f_0 ; b) a high or low decreasing rate of f_0 in the course of dynamic loading; c) a low or high response acceleration that the soil structure can survive; and d) a low or high damping ratio of the structure.

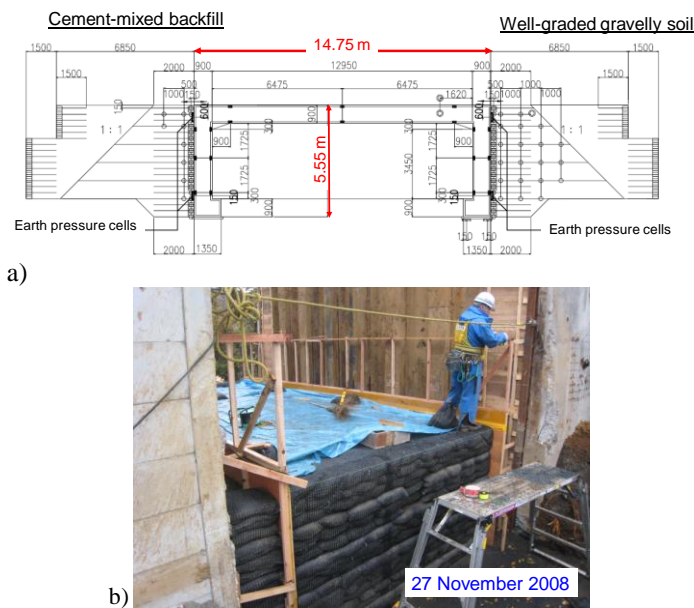


Figure 41. A full-scale model of GRS integral bridge constructed at Railway Technical Research Institute: a) overall structure; and b) the left-side abutment under construction.

6. FULL SCALE MODELS AND PROTOTYPES

6.1 Full-scale models

A full-scale model of GRS integral bridge was constructed during a period of 2008 – 2009 at Railway Technical Research Institute (Fig. 41). The abutments were constructed by excavating the backfill of a pair of full-scale models of GRS-RW with FHR facing constructed in 1988 (Tatsuoka et al., 1997). A high constructability of GRS integral bridge was confirmed. The behaviour during construction was

observed and the long-term behaviour is now being observed.

At the end of 2009, a full-scale model of conventional type bridge was constructed and the backfill of both of the 6.05 m-high abutments was reinforced with 40 cm-diameter nails, then, the 13.31 m-long steel girder was integrated to a pair of abutments (Fig. 42; Suga et al., 2011). A high constructability of this bridge reinforcement method was confirmed.

In January and February of 2012, full-scale lateral loading tests of the GRS integral and NRS integrated bridge models were performed. The results will be reported in the near future.

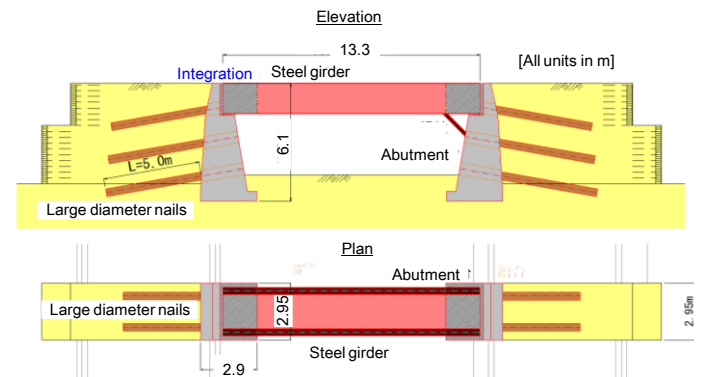
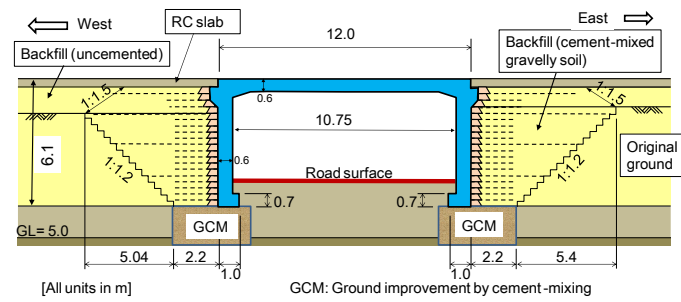


Figure 42. Full-scale model of conventional type bridge reinforced by nailing of the backfill and integrating the girder to the abutments; a) overall structure; and b) a picture of the model immediately after completion (Suga et al., 2011).

6.2 Prototype GRS integral bridge

In 2011, the first prototype GRS integral bridge was constructed at the south end of Hokkaido for a new high-speed train line (Fig. 43). The design maximum train speed is 260 km/h. The estimated construction cost is about a half of the one for a box girder type bridge, which is the most conventional solution in this case (Watanabe, 2011). The bridge is heavily instrumented to observe the behaviour during construction and after opening to service. Several GRS integral bridges for railways, including those reconstructed to restore bridges that collapsed by tsunami during the 2011 Great East Japan Earthquake Disaster, are now at the stage of planning and design.



b)
Figure 43. First GRS integral bridge, Kikonai at the south end of Hokkaido, for a new bullet train line (11.7 m wide): a) overall structure; and b) abutments under construction, summer 2011 (by the courtesy of Japan Railway Construction, Transport and Technology Agency).

6.3 2011 Great East Japan Earthquake Disaster

The girders and approach fills behind the abutment of a great number of road and railway bridges (more than 300) were washed away by tsunami of the 2011 Great East Japan Earthquake Disaster (Kosa., 2012), as typically seen from Figs. 44 - 46. The above was due to the fact that a girder supported by bearings has a very low resistance against uplift and lateral forces of tsunami while the unreinforced backfill is very weak against erosion by over-flow of tsunami. Connectors and anchors that had been arranged to prevent dislodging of the girders from the abutments and piers by seismic loads could not prevent the flow away of the girders by tsunami forces. These cases showed that the bearings and unreinforced backfill are two weak points of the conventional type bridge not only for seismic loads but also for tsunami current.



Figure 44. A view from the seaside of Namiitagawa bridge, between Namiitagawa and Kirikiri stations, Otsuchi-cho, Yamada Line, Iwate Prefecture, East Japan Railway.



Figure 45. A view from the upstream of Tsuyagawa Bridge, between Motoyoshi and Rikuzenkoizumi stations, Kesen-numa line, East Japan Railway.



Figure 46. a) A view from the seaside; and b) the back of the right bank abutment of Yonedagawa bridge, between Rikuchunoda and Rikuchutamagawa stations, Noda village, Iwate Prefecture, North-Rias Line, Sanriku Railway.

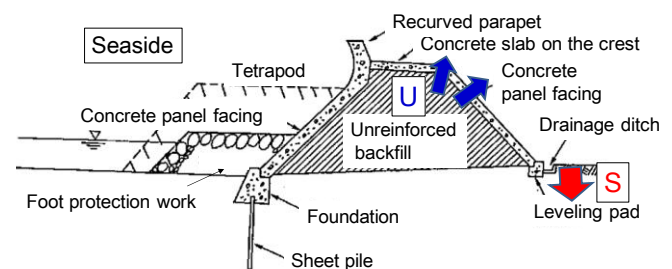


Figure 47. Collapse mechanisms of conventional type coastal dyke by over-flowing tsunami current.

6.4 Proposal of tsunami-resistant bridges and dykes

The resistance against the uplift and lateral forces of tsunami of the girder of GRS integral bridge is substantially higher than the conventional type bridge. This is because the girder of GRS integral bridge is integrated to the facings that are connected to the massive approach fill with geogrid layers, while the approach fill that is reinforced and has full-height rigid facings connected to the geogrid layers is very stable against tsunami current. In this case, the approach fill should also have facings on both sides in parallel of the bridge axis to be stable against tsunami current. Even with GRS integral bridges, neces-

sary provisions should be made for protecting the abutments from scouring in the supporting ground by tsunami current.

Most of conventional type coastal dykes comprise unreinforced backfill with concrete panel facings covering upstream and downstream slopes and crest. When subjected to deep over-flow of tsunami current caused by the 2011 Great East Japan Earthquake Disaster, at many places, the coastal dykes fully collapsed by the following mechanisms (Fig. 45) and had totally lost their function when attached by subsequent tsunamis. Firstly, a strong tsunami current flowing down the down-stream slope scored in the ground in front of the toe of the downstream slope (as denoted by letter 'S' in Fig. 47), by which the concrete facing on the downstream slope was destabilized and washed away; and/or the concrete facings at the crest and the upper part of the downstream slope were peeled off by associated strong uplift forces (as denoted by the letter 'U' in Fig. 47) and washed away. Then, the unreinforced backfill was exposed to tsunami current and eroded quickly from the crest and downstream slope. Subsequently, the drawback of a tsunami damaged the seaside slope by the same mechanism as described above. Finally, the full section disappeared.

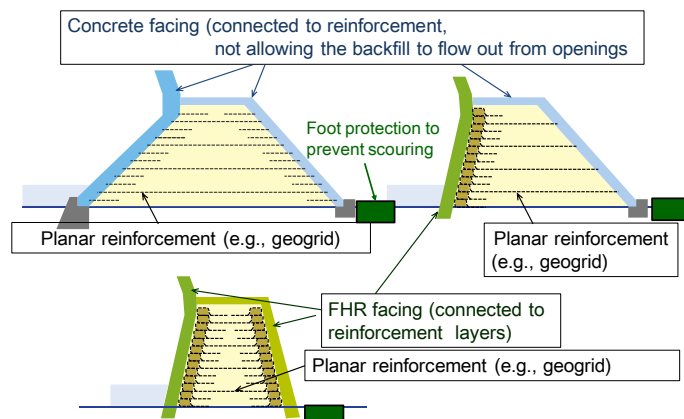


Figure 48. GRS coastal dykes as a tsunami barrier that can survive deep over-flow of tsunami current.

On the other hand, coastal dykes that comprise the geogrid-reinforced backfill with continuous lightly steel-reinforced concrete facings that are firmly connected to the reinforcement, like the GRS RWs illustrated in Fig. 2, should have a much stronger resistance against over-flowing tsunami current. Fig. 48 shows several types that can be proposed at this moment. Yamaguchi et al. (2012) performed a series of small model tests and showed that the stability of these types of GRS coastal dykes (Fig. 48) have a very high resistance against flow away by over-flowing tsunami current, much higher than the ordinary embankment with concrete facing (Fig. 47).

Tatsuoka and Tateyama (2012) proposed to construct GRS integral bridges (Fig. 16) and GRS embankments/dykes (Fig. 48) to restore the conven-

tional type bridges of railways and roads that collapsed by tsunamis of the 2011 Great East Japan Earthquake Disaster. Fig 49 illustrates a proposal for coastal railways. These technologies can also be used to newly construct coastal railways and roads that should survive earthquakes and tsunamis.

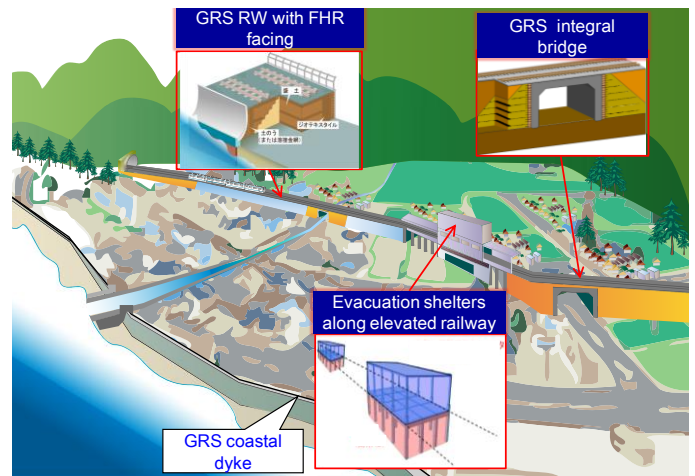


Figure 49. Coastal railway that can survive a great tsunami (Railway Technical Research Institute, Japan, 2011).

7. CONCLUSIONS

Geosynthetic-reinforced soil retaining walls (GRS RWs) having staged-constructed full-height rigid (FHR) facing have been constructed as important permanent RWs for a total length of more than 130 km since 1989 until today in Japan, mainly for railways and also for roads and other types of infrastructure. Its current popular use is due to a high cost-effectiveness with high long-term performance and high seismic stability. This success can be attributed to: i) the use of a proper type of reinforcement (i.e., geogrids for cohesionless soil and nonwoven/woven geotextile composites for high-water content cohesive soil); ii) construction of a FHR facing by such a staged construction procedure that, after the major deformation of the supporting ground and backfill has taken place, fresh concrete is cast-in-place on the wrapped-around wall face of completed geosynthetic-reinforced backfill so that reinforcement layers are firmly connected to the facing; and iii) taking advantage of the rigidity of the facing in design.

A number of embankments and conventional type RWs that collapsed during recent severe earthquakes, heavy rains, floods and storms were reconstructed to GRS RWs of this type. It was validated that this technology is also highly cost-effective in reconstructing collapsed old soil structures.

The GRS integral bridge was developed, which comprises an integral bridge and geosynthetic-reinforced backfill with staged-constructed FHR facing. The results from model tests in the laboratory,

full-scale model tests and construction of a prototype showed the following superior characteristic features over other types of bridge: a) lower cost for construction and maintenance; b) less detrimental effects of seasonal thermal deformation of the girder; and c) a much higher seismic stability. Feature c) is due to: 1) a high initial natural frequency; 2) a low decreasing rate of the natural frequency during dynamic loading; 3) a high energy dissipation capacity at failure; and 4) a high dynamic strength, all by full integration of the girder, the abutments and the reinforced backfill.

It is argued that GRS integral bridges (with geogrid-reinforced approach fill having facings on its three sides) and GRS embankments/dykes with facings connected to the reinforcement also have a very high resistance against tsunami. It is proposed to reconstruct bridges and embankments of railways and roads that collapsed by tsunami of the 2011 Great East Japan Earthquake Disaster to these types of structures. It is also proposed to newly construct tsunami-resistant GRS integral bridges and GRS embankments/dykes for coastal railways and roads.

8. ACKNOWLEDGEMENTS

The authors would like to sincerely thank their previous and current colleagues at the University of Tokyo, Tokyo University of Science and Railway Technical Research Institute, Japan, for their great help to a long-term research performed to develop the GRS technologies described in this paper.

9. REFERENCES

- England, G. L., Neil, C. M. and Bush, D. I. 2000. Integral Bridges, A fundamental approach to the time-temperature loading problem. *Thomas Telford*.
- Kosa, K. 2012. Damage analysis of bridges affected by tsunami due to Great East Japan Earthquake. *Proc. International Sym. on Engineering Lessons Learned from the 2011 Great East Japan Earthquake*, March, Tokyo, Japan, 1386-1397.
- Koseki, J., Bathurst, R.J., Guler, E., Kuwano, J. and Maugeri, M. 2006. Seismic stability of reinforced soil walls. *Proc. 8th International Conference on Geosynthetics, Yokohama*, 1: 51-77.
- Koseki, J., Tateyama, M., Watanabe, K. and Nakajima, S. 2008. Stability of earth structures against high seismic loads." *Keynote Lecture, Proc. 13th ARC on SMGE, Kolkata*, Vol. II.
- Koseki, J. 2012: Use of geosynthetics to improve seismic performance of earth structures. Mercer Lecture 2011. *Geotextiles and Geomembranes*, 34 (2012): 51-68.
- Morishima, H., Saruya, K. and Aizawa, F. 2005. Damage to soils structures of railway and their reconstruction." *Special Issue on Lessons from the 2004 Niigata-ken Chu-Etsu Earthquake and Reconstruction, Foundation Engineering and Equipment (Kiso-ko)*, Oct., 78-83 (in Japanese).
- Munoz, H., Tatsuoka, F., Hirakawa, D., Nishikiori, H., Soma, R., Tateyama, M. and Watanabe, K. 2012. Dynamic stability of geosynthetic-reinforced soil integral bridge. *Geosynthetics International*, 19(1): 11-38.
- Railway Technical Research Institute, Japan. 2011. Technical solutions proposed to restore railways damaged by earthquakes (in Japanese).
- Suga, M., Kuriyama, R., Tateyama, M., Kouda, M., Sugimoto, I. and Kobayashi, Y. 2011. Reinforcing method of bridge by integration of steel girder, abutment and backfill. *Proc. 46th Japan Conf. on Geotechnical Engineering, JGS, Kobe*, Paper No. H-06, pp.1499-1500 (in Japanese).
- Tateyama, M., Tarumi, H. and Fukuda, A. 1996. Development of a large diameter short reinforced anchor by cement-mixing method, *Grouting and Deep Mixing, Proc. cond Int. Conf. on Ground Improvement Geosystems, Tokyo*, pp. 759-765.
- Tateyama, M. 2012. Damage to railways by the 2011 Great East Japan Earthquake *Geosynthetics Engineering Information*, 28(1), March: 1-8 (in Japanese).
- Tatsuoka, F. 1992. Roles of facing rigidity in soil reinforcing. *Keynote Lecture, Proc. Earth Reinforcement Practice, IS-Kyushu '92 (Ochiai et al. eds.)*, 2: 831-870.
- Tatsuoka, F., Tateyama, M., Uchimura, T. and Koseki, J. 1997. Geosynthetic-reinforced soil retaining walls as important permanent structures. *Mercer Lecture, Geosynthetic International*, Vol.4, No.2, pp.81-136.
- Tatsuoka, F., Koseki, J., Tateyama, M., Munaf, Y. and Horii, N. 1998. Seismic stability against high seismic loads of geosynthetic-reinforced soil retaining structures." *Keynote Lecture, Proc. 6th Int. Conf. on Geosynthetics, Atlanta*, 1: 103-142.
- Tatsuoka, F., Tateyama, M., Aoki, H. and Watanabe, K. 2005. Bridge abutment made of cement-mixed gravel backfill. *Ground Improvement, Case Histories, Elsevier Geo-Engineering Book Series, Vol. 3* (Indradratna & Chu eds.), 829-873.
- Tatsuoka, F., Tateyama, M., Mohri, Y. and Matsushima, K. 2007. Remedial treatment of soil structures using geosynthetic-reinforcing technology. *Geotextiles and Geomembranes*, 25 (4 & 5): 204-220.
- Tatsuoka, F., Hirakawa, D., Nojiri, M., Aizawa, H., Tateyama, M. and Watanabe, K. 2008a. Integral bridge with geosynthetic-reinforced backfill. *Proc. First Pan American Geosynthetics Conference & Exhibition, Cancun, Mexico*, 1199-1208.
- Tatsuoka, F., Hirakawa, D., Aizawa, H., Nishikiori, H., Soma, R. and Sonoda, Y. 2008b. Importance of strong connection between geosynthetic reinforcement and facing for GRS integral bridge. *Proc. 4th GeoSyntheticsAsia (4th Asian Regional Conference on Geosynthetics)*, Shanghai.
- Tatsuoka, F., Hirakawa, D., Nojiri, M., Aizawa, H., Nishikiori, H., Soma, R., Tateyama, M. and Watanabe, K. 2009. A new type integral bridge comprising geosynthetic-reinforced soil walls. *Geosynthetics International, IS Kyushu 2007 Special Issue*, 16(4): 301-326.
- Tatsuoka, F., Koseki, J. and Tateyama, M. 2010a. Introduction to Japanese codes for reinforced soil design, Panel Discussion on Reinforced Soil Design Standards, *Proc. 9th International Conference on Geosynthetics, Brazil*, 245-255.
- Tatsuoka, F., Hirakawa, D., Nojiri, M., Aizawa, H., Nishikiori, H., Soma, R., Tateyama, M. and Watanabe, K. 2010b. Closure to Discussion on "A new type of integral bridge comprising geosynthetic-reinforced soil walls." *Geosynthetics International*, 17(4): 1-12.
- Tatsuoka, F., Kuroda, T. and Tateyama, M. 2012a. Research and practice of GRS integral bridges, *Proc. EuroGeo 5, Valencia*, September (to appear).
- Tatsuoka, F., Munoz, H., Kuroda, T., Nishikiori, H., Soma, R., Kiyota, T., Tateyama, M. and Watanabe, K. 2012b. Stability of existing bridges improved by structural integration and nailing, *Soils and Foundations*, 52(3) (to appear).

- Tatsuoka, F. and Tateyama, M. 2012. Geosynthetic-reinforced soil structures for railways in Japan, Keynote Lecture, *Proc. International Conference on Ground Improvement and Ground Control (ICGI 2012)* (Indraratna et al., eds.)
- Watanabe, K. 2011. Application of GRS integral bridge technology to Hokkaido High-Speed Train Line (Shinkansen). *Journal of Japan Railway Civil Engineering Association*, 49(10): 83-86 (in Japanese).
- Yamaguchi, S., Yanagisawa, M., Uematsu, Y., Kawabe, S., Tatsuoka, F. and Nihei, Y. 2012. Experimental evaluation of the stability of GRS coastal dyke against over-flowing tsunami. *Proc. 47th Japan Conf. on Geotechnical Engineering, JGS, Hachinohe* (in Japanese).